The first multi-model ensemble of regional climate simulations at kilometer-scale resolution part 2: historical and future simulations of precipitation

Emanuela Pichelli[1] · Erika Coppola[1] · Stefan Sobolowski[2] · Nikolina Ban[3] · Filippo Giorgi[1] · Paolo Stocchi[4] · Antoinette Alias[5] · Danijel Belušić[6] · Segolene Berthou[7] · Cecile Caillaud[5] · Rita M. Cardoso[8] · Steven Chan[7,9] · Ole Bøssing Christensen[10] · Andreas Dobler[11] · Hylke de Vries[12] · Klaus Goergen[13] · Elizabeth J. Kendon[7] · Klaus Keuler[14] · Geert Lenderink[12] · Torge Lorenz[2] · Aditya N. Mishra[15] · Hans-Juergen Panitz[16] · Christoph Schär[17] · Pedro M. M. Soares[8] · Heimo Truhetz[15] · Jesus Vergara-Temprado[17]

Abstract

This paper presents the first multi-model ensemble of 10-year, "convection-permitting" kilometer-scale regional climate model (RCM) scenario simulations downscaled from selected CMIP5 GCM projections for historical and end of century time slices. The technique is to first downscale the CMIP5 GCM projections to an intermediate 12–15 km resolution grid using RCMs, and then use these fields to downscale further to the kilometer scale. The aim of the paper is to provide an overview of the representation of the precipitation characteristics and their projected changes over the greater Alpine domain within a Coordinated Regional Climate Downscaling Experiment Flagship Pilot Study and the European Climate Prediction system project, tasked with investigating convective processes at the kilometer scale. An ensemble of 12 simulations performed by different research groups around Europe is analyzed. The simulations are evaluated through comparison with high resolution observations while the complementary ensemble of 12 km resolution driving models is used as a benchmark to evaluate the added value of the convection-permitting ensemble. The results show that the kilometer-scale ensemble is able to improve the representation of fine scale details of mean daily, wet-day/hour frequency, wet-day/hour intensity and heavy precipitation on a seasonal scale, reducing uncertainty over some regions. It also improves the representation of the summer diurnal cycle, showing more realistic onset and peak of convection. The kilometer-scale ensemble refines and enhances the projected patterns of change from the coarser resolution simulations and even modifies the sign of the precipitation intensity change and heavy precipitation over some regions. The convection permitting simulations also show larger changes for all indices over the diurnal cycle, also suggesting a change in the duration of convection over some regions. A larger positive change of frequency of heavy to severe precipitation is found. The results are encouraging towards the use of convection-permitting model ensembles to produce robust assessments of the local impacts of future climate change.

1 Introduction

Regional Climate Models (RCMs) are useful tools to explore climate at refined scales compared to global models (Giorgi 2019), although they still maintain a degree of error and uncertainty related to sub-grid processes that are approximated through parameterizations. The added value derived from the resolution enhancement of RCMs is not obvious, since it may depend on different factors such as the variable of interest, the complexity of the region of application, the experiment configuration, model parameterizations, etc. (Torma et al. 2015; Prein et al. 2015). It has been shown, however, that increased horizontal resolution generally improves the representation of fine scale processes and is particularly useful in areas with complex terrain for better

✉ Emanuela Pichelli
epichell@ictp.it

Extended author information available on the last page of the article

simulating the topographical forcing on precipitation (Rasmussen et al. 2014; Torma et al. 2015; Pontoppidan et al. 2017).

Today, the rapid increase in computing power allows one to push the model horizontal resolution toward the kilometer-scale even for climate simulations. This enables researchers to investigate and assess climatic changes at regional to local scales and to study related fine scale processes. The resolution increase alone, however, does not guarantee improved representation of precipitation at daily to sub-daily time scales (Dirmeyer et al. 2012). For example, Fosser et al. (2019) show that, at the convection-permitting scale, improvements on the sub-daily precipitation representation are consistently obtained, but the added value due to resolution may decrease at a very fine scale (< 2 km) and the sensitivity to the representation of physical processes can have similar impacts. As another example, Brockhaus et al. (2008) demonstrated the negative impact that the underestimated representation of convective processes can have on the evolution of diurnal atmospheric profiles.

In this context it appears clear that there are advantages of using RCMs at the so-called "convection permitting" or "kilometer" scales, i.e. at a resolution high enough (≤ 4 km) to allow an explicit treatment of deep convection without the use of convection parameterization schemes. A number of studies have presented applications at the kilometer-scale (hereafter referred to as km-scale) resolution (Kendon et al. 2012, 2017; Chan et al. 2013, 2016, 2020; Ban et al. 2014, 2015; Prein et al. 2015, 2017a; Fosser et al. 2015, 2017; Berthou et al. 2018; Fumière et al. 2019; Coppola et al. 2020a), demonstrating the added value of such simulations in realistically representing precipitation over small spatial and temporal scale.

Fewer studies have focused on climate change projections using convection-permitting simulations and these have mostly been single model experiments. Previous research has highlighted that ensemble approaches lead to more robust assessments of climate change both at the global and regional scale (Gleckler et al. 2008; Jacob et al. 2014, 2020), since different models can present different responses to climate forcings, thereby introducing substantial uncertainties in the projected change signals. A downside to conducting climate-scale numerical experiments (e.g. 10 years or more) at km-scales is that computational costs and data volume/handling can be prohibitive. A few studies employed a two model approach (Berthou et al. 2018) or have attempted to synthesize across multiple regions/studies (Kendon et al. 2017). Recently, an ensemble of twelve km-scale projections were carried out as part of the UK Climate Projections project (Kendon et al. 2019). These ensembles can provide an initial estimate of uncertainties in future changes at km-scale, but they only sample uncertainty in the driving model physics and not in the convection-permitting model itself.

To date no study has investigated changes in precipitation characteristics in a coordinated large multi-model km-scale framework.

Therefore, a Coordinated Regional Climate downscaling Experiment Flagship Pilot Study (CORDEX-FPS) initiative was organized to investigate present and projected convective processes over Europe, and more specifically the greater Alpine region, at the km-scale (Coppola et al. 2020a). A number of experiments have been planned within the CORDEX-FPS, some also contributing to the European Climate Prediction System (EUCP) project. The first focused on test cases (Coppola et al. 2020a), while another focused on 10-year ERA-Interim driven evaluation simulations (Ban et al. 2021). A third experiment, which is the focus of this paper, consists of multi-model 10-year km-scale scenario simulations downscaled from selected CMIP5 GCM projections for three time slices (historical, mid 21st century and end of 21st century). The goal here is thus to present the first overview of the representation of precipitation and its projection over the greater Alpine domain in this multi-model experiment and to assess the advantages of using convection-permitting models in a climate change context.

Three short sections introduce the experimental design, the observational dataset and the analysis method. Then, an assessment of the performance of the multi-model ensemble at the convection permitting scale (CPRCM) is presented by comparison of the historical period simulations with high resolution observations, also comparing the results with the ensemble of the coarser resolution driving regional climate models (RCMs) as a benchmark to evaluate the added value of this convection permitting set of simulations. A section on the analysis of the end-of-century projection follows and finally the last section provides a summary and main conclusions. Figures (S1–S7) dedicated to the daily scale analysis are provided in the supplementary material of the paper.

2 Experiment design and ensemble description

We use a subset of simulations performed within the CORDEX-FPS. These simulations are all run at convection-permitting resolutions that do not require the use of deep cumulus parameterizations and at least partially resolve convective phenomena (Prein et al. 2015; Coppola et al. 2020a). The ensemble considered here consists of 12 high-resolution simulations (2–3 km, CPRCM), performed with 5 different RCMs, over domains that must encompass the greater Alpine region shown in Fig. 1, which is our analysis region.

The full list of models and institutes that carried out the simulations is reported in Table 1. The CPRCMs, with exception of the UM simulation run by the UK Met Office, are run with intermediate resolution RCMs (12–15 km) with
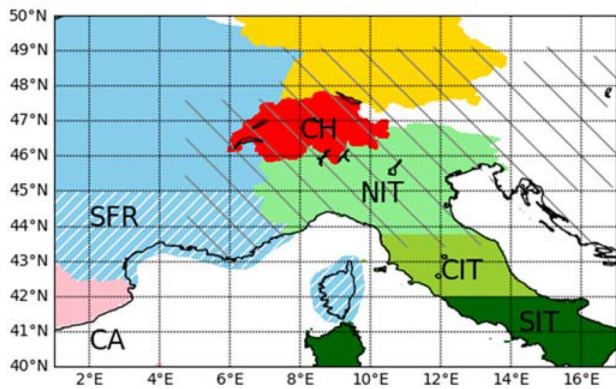
Fig. 1 Common domain (CA). Areas where observed dataset are available (Sect. 3) are in different colours: EURO4M-APGD (dashed grey), REGNIE (yellow), Spain02 (pink), RdisaggH (red), COME-PHORE (blue), GRIPHO (greenish). Sub-domain areas considered in the analysis are labelled: South France (SFR), North, Central, South Italy (N/C/SIT), Switzerland (CH)

domains that cover all of Europe and the use of convection parameterizations to account for convection. They serve both as driving models and benchmarks for comparison. The RCMs are driven by GCMs participating in the CMIP5 program (Taylor et al. 2012), except for ETHZ(b), which utilizes a "pseudo-global-warming" (PGW) approach. In short, this approach simulates climate with driving fields from the ERA-Interim reanalysis and adds the forced warming signal from a climate projection obtained from a GCM (Schär et al. 1996; Rasmussen et al. 2011; Liu et al. 2017; Hentgen et al. 2019).

The experiments set for the CORDEX-FPS consist of 10-year simulations of selected CMIP5 GCM projections for three time slices: 1996–2005, 2041–2050, 2090–2099 (historical, mid-century and end-of-century, respectively) under the rcp8.5 scenario (Moss et al. 2010). Each time slice has at least one year of spin-up previous to the indicated period. Only the historical and end-of-century time slices of the scenario simulations are investigated for this study, as the mid-century simulations are still under way.

Table 1 Contributing models (CPRCMs and driving intermediate RCMs)

Institute	CPRCM	Resolution (km)	Driving RCM	Resolution (km)	GCM
KNMI (*) The Royal Netherlands Meteorological Institute	HCLIM38-AROME (A)	2.5	RACMO	12	EC-Earth
ICTP (*) Abdus Salam International Centre for Theoretical Physics-Earth System Physics	RegCM4 (B)	3	RegCM4 (B)	12	HadGEM
CNRM (*) Centre National de Recherches Meteorologique	CNRM-AROME41t1 (C)	2.5	CNRM-ALADIN63 (Euro-COR-DEX) (C1)	12	CNRM-CM5
KIT Karlsruhe Institute of Technology	CCLM5 (D)	3	CCLM4 (D1)	12	MPI-ESM-LR
BTU Brandenburg University of Technology	CCLM5 (D)	3	CCLM4 (Euro-CORDEX) (D1)	12	CNRM-CM5
ETHZ(a, *) Federal Institute of Technology, Institute for Atmospheric and Climate Science	CCLM	2.2	CCLM	12	MPI
ETHZ(b, *) Federal Institute of Technology	CCLM	2.2	CCLM	12	pgw
FZJ-IBG3 IDL Research Centre Julich Institute Dom Luis	WRF3.8 (E)	3	WRF3.8.1CA (Euro-CORDEX)	15	EC-EARTH
DMI- MET Norway- SMHI (*) HARMONIE-Climate community	HCLIM38-AROME (A)	3	HCLIM38-ALADIN (A)	12	EC-EARTH
UNIGRAZ-WEGC Wegener Center for Climate and Global Change, University of Graz	WEGC-CCLM5 (D)	3	WEGC-CCLM5 (Euro-CORDEX) (D1)	12	MPI-ESM-LR
UK Met OFFICE (*) Met Office Hadley Centre Exeter	UM (F)	2.2	No intermediate RCM		HadGEM
BCCR The Bjerknes Centre for Climate Research	WRF3.8	3	WRF3.8.1CA (Euro-CORDEX)	15	NorESM1

References: (A) Belušić et al. (2020); (B) Giorgi et al. (2012), Coppola et al. (2020a), (C) Caillaud et al. (2020), (C1) Nabat et al. 2020; (D) Rockel et al. (2008), Baldauf et al. (2011); (D1) Keuler et al. (2016); (E) Powers et al. (2017), (F) Berthou et al. (2018), Chan et al. (2019)

The starred CPRCMs (*) are contributing to EUCP project. CPRCMs have different domain size but all cover the common Alpine region as in Fig. 1. RCMs domains cover Europe and have generally different sizes, except the ones flagged as Euro-CORDEX

Prior to the analysis, hourly precipitation data from the CPRCM ensemble members are remapped onto a common grid with 3 km resolution and their driving RCMs are remapped onto a 12 km common grid. The only exception to this procedure is the UM simulation, which is only remapped to the 3 km grid, directly downscaled from a 25 km HadGEM simulation.

3 Observation datasets

Our analysis domain covers the Alpine region and surrounding areas (Fig. 1). There is no single high resolution observation dataset that covers the entire analysis domain, and therefore the assessment of the ensemble for the historical period consists of a comparison with a number of different high-resolution (space and time) observation-based precipitation datasets available over different areas: Alps, France, Italy, Germany, Switzerland (Fig. 1). The time period considered for the analysis against observations is the same as the simulated historical period (1996–2005), unless otherwise specified. A brief summary of the datasets and their spatial and temporal coverage is provided below:

- EURO4M-APGD: daily precipitation data available at a horizontal grid spacing of 5 km over the Alpine region. This data set is based on daily rain gauge station data (Isotta et al. 2014);
- REGNIE: gridded dataset of daily precipitation available on a 0.02 × 0.008 deg horizontal grid-spacing comprising the regionalization of all existing DWD precipitation data (Rauthe et al. 2013);
- Spain02: gridded daily precipitation dataset built including ~ 2500 quality-controlled stations over Spain at ~ 12 km grid spacing (Herrera et al. 2010);
- E_OBS: 0.25 degree gridded dataset of daily precipitation derived from wide station network (Cornes et al. 2018);
- RdisaggH: gridded hourly precipitation data, available over the area of Switzerland with a horizontal grid spacing of 1 km (Wuest et al. 2010), available for the period 2003–2010. It is based on a combination of station data and it is disaggregated using radar data. This dataset is used only for the hourly precipitation analysis;
- GRIPHO: gridded hourly precipitation data, available over Italy with a horizontal grid spacing of 3 km, based on rain gauge data (Fantini, 2019). These data are available for the period 2001–2016 and are here considered for the decade 2001–2010;
- COMEPHORE: hourly observational dataset at 1 km grid spacing available over France (Fumière et al. 2019; Tabary et al. 2012) and produced through a combination

of radar and rain gauge data. We here consider the decade 1997–2006.

The observations are maintained on their original resolution, unless some bias is computed. In this case, the models are remapped to the observation grid if this is at a coarser resolution or vice versa if the observed dataset has a greater resolution than the model's.

Despite the high spatial and temporal resolution of these datasets, it is important to recognize some shortcomings, such as the underestimation of precipitation over mountainous regions due to the sparseness of stations and the masking effects of radars, the systematic wind-induced rain gauge under-catch (La Barbera et al. 2002), and wetting/evaporation losses. Additionally, gridded datasets are typically produced using interpolation methods, which induces an underestimation of high intensities (smoothing effect) and overestimation of low intensities (moist extension into dry areas) (Isotta et al. 2014).

Prein and Gobiet (2017) demonstrated that the spread of observation datasets from different sources are often comparable with the spread of model ensembles, at least at the 0.11° horizontal grid spacing used for the intermediate resolution ensemble. This is in line with previous findings at the global scale (Herold et al. 2015). The high density of stations within a grid cell is a key issue to reduce the uncertainty of the dataset (Isotta et al. 2015; Prein and Gobiet 2017) and the recommendation for model studies is thus to consider ensembles of observational data sets instead of data from a single source (Prein and Gobiet 2017). In the present study we use the highest resolution dataset available for each sub-region considered in order to maximize the station density, thus minimizing the uncertainty for that area (as for the regional dataset in Prein and Gobiet 2017, see their Fig. 11). One exception to this criterion is the GRIPHO dataset for southern Italy, where the station density is not as high as in the north. Some other datasets, such as COMEPHORE and RdisaggH, are composite of both gauge and radar information, which is a promising technique to increase the accuracy of measurements (Prein and Gobiet 2017).

For the datasets that do not overlap completely with the historical simulation period we included 10-years if available, or the longest possible time series. Because of this lack of perfect overlap between time periods, we do not expect a perfect comparison between observations and models but aim to assess the ensemble's first order performance. It should also be noted that the driving GCMs of the ensemble do not preserve the observed low frequency variability because they do not include assimilation of observations and only follow external 20th century forcing. Therefore, the temporal overlap with observations is of relatively low importance and the comparison can be done only in a statistical way, rather than on an event or year-by-year basis.

4 Statistical indices

A number of statistical indices are used to evaluate the models' ability to reproduce the observed precipitation climatology and assess the impact of projected climate change. The indices are calculated on a seasonal basis considering the triplet June–July–August (JJA) for summer and September–October–November (SON) for autumn.

Defining a wet-day as a day with at least 1 mm of rain and a wet-hour as an hour with at least 0.1 mm of rain, the indices used are:

- Mean daily precipitation (mm/day)
- Wet-day/hour frequency (fraction of number of wet-days per season)
- Wet-day/hour intensity (mm/day or mm/h)
- Heavy precipitation defined as the 99th or 99.9th percentile (p99, p99.9) of all daily or hourly precipitation events (mm/day or mm/h)
- Probability density function (PDF) defined as the normalized frequency of occurrence of precipitation events within a certain bin.

5 Results

Our assessment focuses on the JJA and SON seasons, since convective events and processes dominate in these seasons over the region of interest. For the summer season the focus is on precipitation processes that are primarily driven by thermal convective forcing across the Alpine region. During autumn the Alps and in general the surrounding Mediterranean areas are often affected by heavy precipitation events that, especially when occurring over small and steep river catchments typical of the area, can result in disastrous floods (Ducrocq et al. 2014).

5.1 Assessment of the reference period (1996–2005)

5.1.1 Hourly scale assessment

Mean summer and autumn wet-hour intensity (> 0.1 mm/hour), wet-hour frequency and heavy hourly precipitation (i.e. the 99.9th percentile of all events) are shown in Figs. 2 and 3, respectively. The ensemble averages of the CPRCMs and the intermediate RCMs are shown in the mid and right columns respectively, while the combined high-resolution observation data available at hourly frequency (Sect. 3) are used for the model assessment over Italy, France and Switzerland.

The CPRCM ensemble generally better represents all the indices at the hourly scale (Figs. 2 and 3, top row), improving the representation found in the driving RCM ensemble in both seasons. An increase in detail is seen with increasing resolution, clearly related to the refined representation of topography in the CPRCM ensemble and the resulting interactions between (thermo)dynamical processes and orography.

In JJA (Fig. 2) the driving RCM ensemble produces weak (underestimated) but very frequent (overestimated) precipitation events, especially across the alpine chain. Correspondingly, the CPRCM ensemble reduces the disagreement with observations (RCM intensity percent bias: − 20/− 70% (minimum and maximum ranges); CPRCM: − 10/− 20% across southern France and the Swiss Alps; + 5/+ 40% elsewhere; not shown), improving weak to moderate precipitation and reducing the precipitation frequency (Fig. 2, top and middle row). The biases with respect to the highest resolution observation (HR-OBS) across some sub-areas of interest (Fig. 1, CH, SFR, NIT, CIT, SIT) are reported in Table 2, which shows a reduction of error over most areas.

The spread of the CPRCM and driving RCM ensembles for the indices analyzed is shown in Fig. 4 for both seasons over the entire analysis area (CA on Fig. 1) and the sub-areas of interest. The bar plots show the 5th, 25th, 75th and 95th percentiles, median (black) and mean (yellow), while models falling outside these limits are plotted as single points. For each area, the highest resolution observation (HR-OBS) is reported. Despite the bias reduction, the box-plots show a larger spread in hourly precipitation intensity for the CPRCM ensemble than the RCM one (Fig. 4, top row). Conversely, for the wet-hour frequency (Fig. 4, second row) the CPRCM ensemble shows a much lower spread over most sub-regions.

The improvements by the CPRCM are even more evident when considering heavy precipitation events (Fig. 2, bottom row). Specifically, the CPRCM ensemble considerably improves the underestimation of the wettest events shown by the driving RCMs, showing a good comparison with observations in terms of spatial distribution, especially over the alpine maxima.

The two ensembles (Fig. 4, third row) have similar spreads between the first and third quartile, while the CPRCMs show greater uncertainty within the 5th and 95th percentile. Reduced biases (Table 2) are found on average over all areas for the CPRCM ensemble.

Overall, the comparison with observations for summer, i.e. when precipitation is mostly related to thermal convective forcing, highlights the added value of the CPRCMs with respect to the models using convection parameterizations.

Similar considerations are drawn for SON (Fig. 3), although a larger intensity bias is found for the CPRCMs
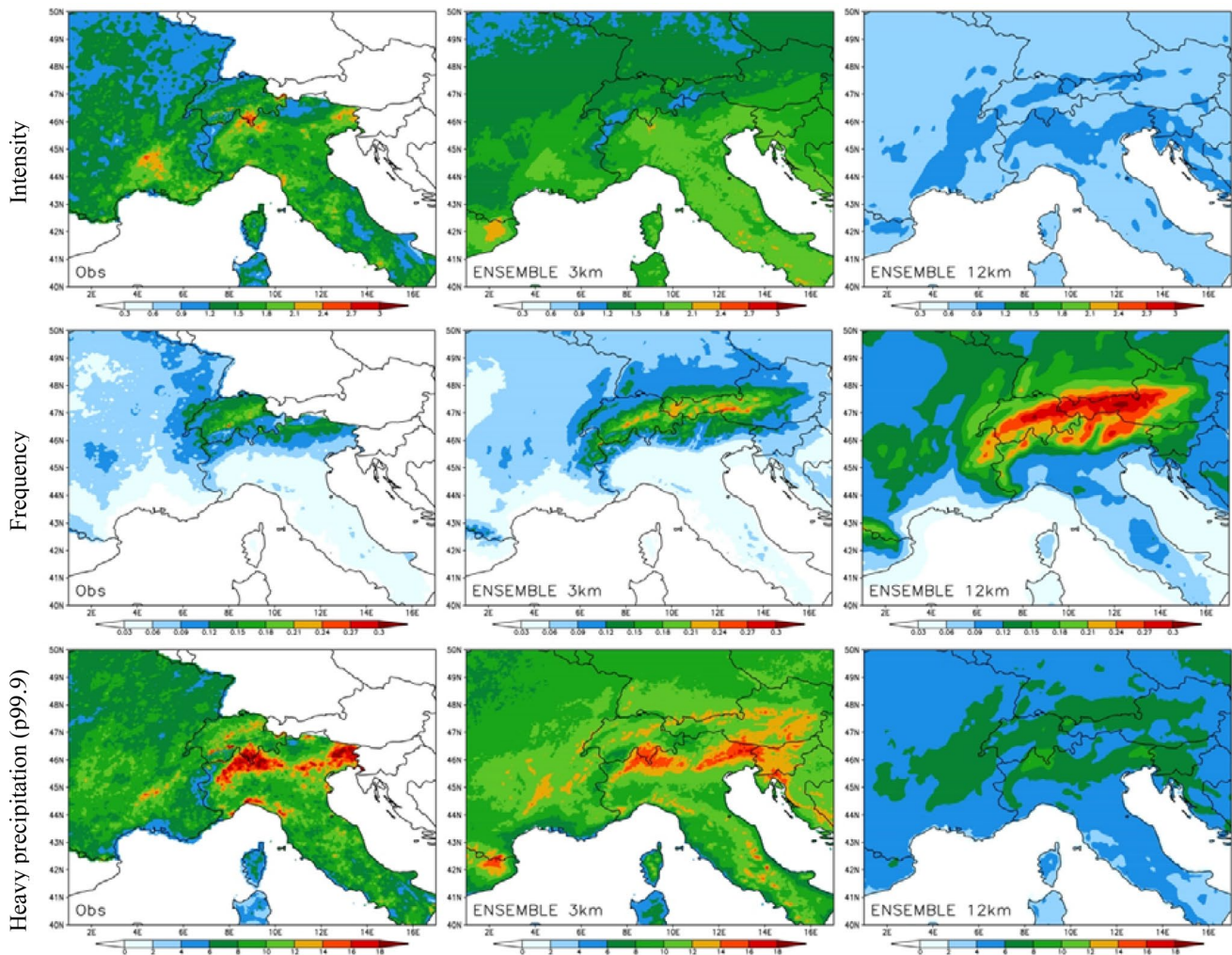
Fig. 2 Summer hourly indices over the Alpine region. From top to bottom: intensity of hourly precipitation (mm/h), wet-hour frequency, heavy hourly precipitation (mm/h) events (p99.9). Results are obtained (from left to right) by a combination of high resolution observations over different areas (see Sect. 3 for details and considered periods), the ensemble of CPRCMs and the ensemble of the corresponding driving RCMs. The model results are averaged over the period 1996-2005

in some areas (RCM intensity bias: − 10/− 70%; CPRCM: − 10/− 40% over France and Switzerland; 5–40% over Italy, not shown). The frequency of wet events (Fig. 3, middle) is still overestimated with respect to observations even at the km-scale, especially across the Alpine mountains. However, unlike JJA, the CPRCMs show a lower spread than the RCM ensemble for this index (Fig. 4, second row, right). In addition, the bias with respect to observations (Table 2) is reduced over NIT and SFR, which are among the regions mostly affected by the occurrence of extreme precipitation episodes in autumn.

The CPRCM ensemble shows a better ability than the driving RCMs in simulating heavy hourly precipitation events (Fig. 3, bottom), with a reliable representation across the Alps and the Mediterranean coasts. In fact, the added

value of the high CPRCM resolution is most evident in these areas, where the precipitation forcing is the result of complex mesoscale interactions between orography, land–ocean interfaces, large-scale circulations and convective processes that are likely more realistically represented at high resolutions. Moreover, Fig. 4 (bottom) highlights a lower spread in SON for the CPRCM ensemble than for RCMs and a general tendency among ensemble members to overestimate extremes in this season.

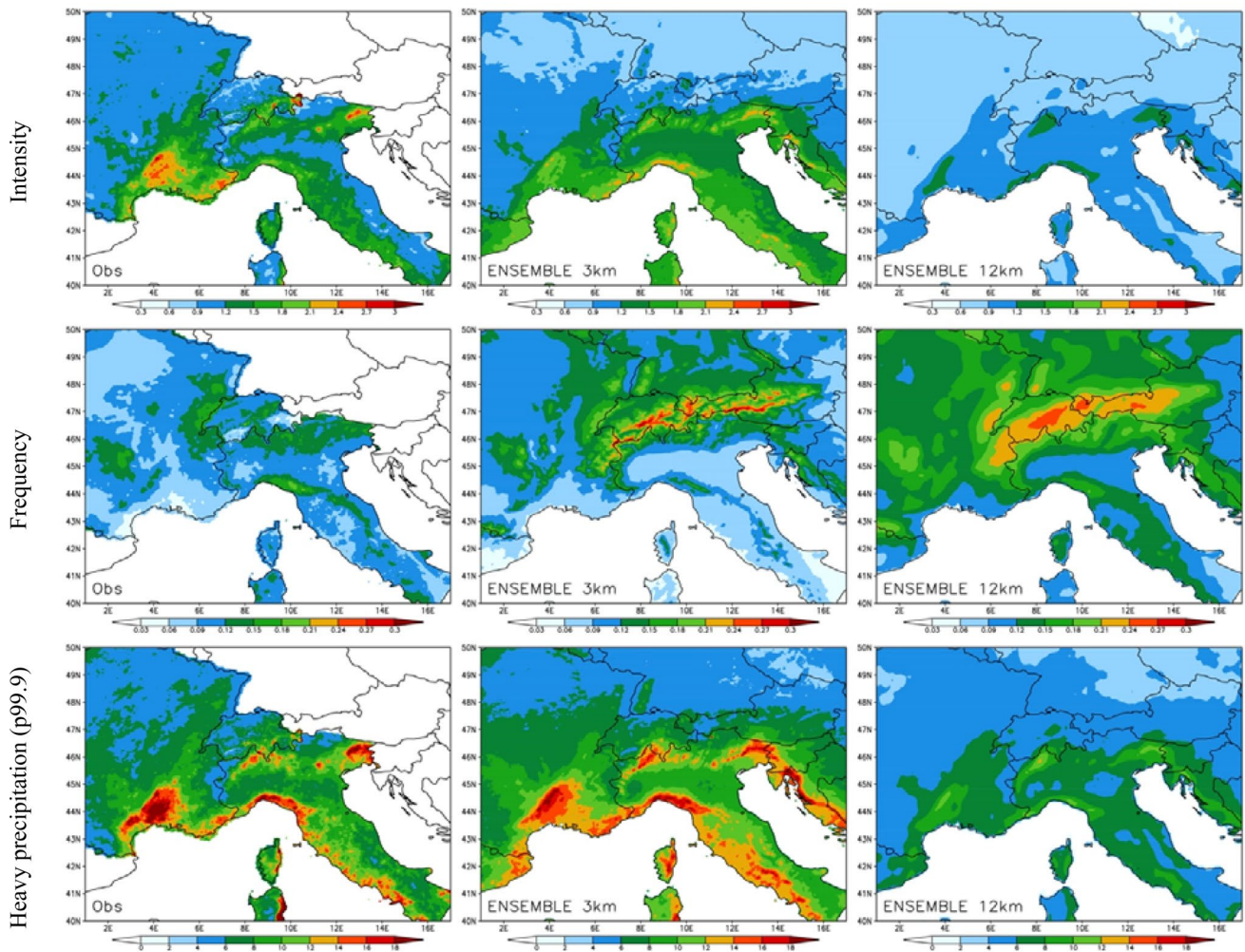Overall, the behavior of the two ensembles at the subdaily scale is maintained at the daily scale, as discussed below.

Fig. 3 As Fig. 2 but for autumn hourly precipitation (mm/h)

5.1.2 Daily scale assessment (supplementary material)

Results for the daily metrics are available in the supplementary material of the paper. The summer and autumn indices over the historical period analysis are presented in Fig. S1 and S2, respectively. Overall, the CPRCM ensemble tends to overestimate local mean daily precipitation maxima in all seasons, but to reproduce a realistic spatial distribution of precipitation and fine scale details compared to the observations. In JJA, the CPRCM ensemble exhibits a reduced mean daily precipitation bias (10–30% less) compared to the coarser resolution RCM ensemble, especially around high mountain areas. In SON, the CPRCM ensemble reduces biases across southern Germany, around main orography in southern France, and across the northern Apennines in northern Italy. The autumn daily precipitation over these areas is in fact underestimated by the intermediate RCMs ensemble. At the same time, the CPRCM ensemble worsens the precipitation overestimation over the western Alps already found in the driving RCMs.

The spread of the two ensembles for the daily indices is shown in figure S3, where mean values are compared with HR-OBS and other lower resolution observations available on each area (Sect. 3). For the mean precipitation (Fig. S3, top row) the two ensembles show comparable spreads in JJA, and for some regions (NIT, SFR) the CPRCMs are distributed around the HR-OBS average, whereas the majority of 12-km RCMs produce an overestimation. For each sub-region the available observations may show differences among datasets, which are significant for datasets with very different resolutions (E_OBS and HR-OBS or E_OBS and EURO4M-APGD). In SON, the CPRCM ensemble shows a smaller spread over the Alpine area (CH, NIT), but a large uncertainty elsewhere. Biases in Table 2 confirm a prevailing reduction of the errors by the CPRCM ensemble.

Table 2 Biases between ensembles (3 km CPRCMs and 12 km RCMs) and observations for analysed indices averaged over sub-areas (as in Fig. 1, CH: Switzerland, (N/C/S)IT:(North/Central/South) Italy, (S)FR: (South) France) where high resolution observed dataset are available (Sect. 3) for JJA and SON over the historical period 1996–2005

1996–2005	CH		IT		NIT		CIT		SIT		FR		SFR	
	3 km	12 km	3 km	12 km	3 km	12 km	3 km	12 km	3 km	12 km	3 km	12 km	3 km	12 km
JJA														
Mean PR-d	0.31	0.19	0.19	0.35	0.16	0.48	0.11	0.13	0.21	0.15	0.18	0.30	0.27	0.41
INT-d	0.49	− 1.55	0.74	− 1.44	0.21	− 1.58	0.74	− 1.82	1.70	− 1.00	0.88	0.61	0.99	− 1.00
FREQ-d	− 0.01	0.07	− 0.01	0.07	− 0.01	0.09	− 0.01	0.05	− 0.01	0.04	− 0.02	0.05	0.00	0.06
P99-d	0.75	− 6.13	1.71	− 2.22	0.11	− 2.83	1.81	− 3.10	4.00	− 1.29	3.09	− 0.10	1.73	− 1.50
INT-h	− 0.09	− 0.62	0.28	− 0.66	0.14	− 0.70	0.31	− 0.71	0.54	− 0.53	0.10	− 0.49	0.12	− 0.61
FREQ-h	0.01	0.09	0.00	0.05	0.00	0.07	− 0.01	0.04	− 0.01	0.03	0.00	0.05	0.00	0.05
P99.9-h	0.35	− 4.05	0.60	− 4.32	0.04	− 5.03	0.60	− 4.37	1.51	− 3.08	1.61	− 2.16	1.30	− 2.50
SON														
Mean PR-d	1.78	1.36	− 0.04	− 0.25	0.14	− 0.10	− 0.13	− 0.34	− 0.40	− 0.55	0.17	0.08	0.10	− 0.04
INT-d	1.44	− 0.25	0.75	− 1.86	0.44	− 2.26	1.02	− 1.61	1.00	− 1.46	0.34	− 0.89	0.40	− 2.05
FREQ-d	0.11	0.13	− 0.03	0.02	0.00	0.04	− 0.04	0.01	− 0.06	− 0.02	0.00	0.03	− 0.01	0.04
P99-d	9.83	2.25	1.47	− 6.74	0.76	− 7.40	3.86	− 5.40	0.22	− 7.39	2.39	− 1.53	2.28	− 5.92
INT-h	− 0.16	− 0.39	0.28	− 0.30	0.19	− 0.29	0.35	− 0.35	0.43	− 0.30	− 0.10	− 0.43	− 0.03	− 0.58
FREQ-h	0.07	0.10	− 0.02	0.02	− 0.01	0.03	− 0.02	0.02	− 0.04	0.01	0.01	0.05	0.00	0.05
P99.9-h	0.34	− 1.65	1.38	− 2.94	1.20	− 2.36	1.85	− 3.39	1.43	− 3.77	0.83	− 1.76	1.41	− 3.09

Flag "d" and "h" refer to daily and hourly indices

The CPRCM ensemble simulates better the intensity of the wet-day precipitation (Figures S1 and S2, second row), improving the underestimation found in the driving RCMs in both JJA and SON. For the main observed maxima in JJA wet-day intensity (Fig. S1, second row, areas around 46 N, 9E and 46 N, 14E), the negative bias exhibited by the 12 km RCMs (ranging between − 20 and − 40% in those locations) is approximately halved. The two ensembles show opposite area averaged biases (Table 2) across regions surrounding the Alps (CH, NIT) and reduced values for the CPRCMs.

In SON the mean wet-day intensity produced by the CPRCM ensemble (Fig. S2, second row) compares well with observations especially over the orographic regions across the Mediterranean, frequently affected by disastrous weather events during this season. Maxima produced by the CPRCMs appear much more realistic compared with observations. Both ensembles exhibit a positive wet day intensity bias across the north side of the Alps chain (5–40%) and negative biases in the surrounding areas, although strongly reduced by the CPRCMs (− 40/− 20% for RCMs, − 5/− 20% for CPRCMs). Moreover, the CPRCM ensemble reverses the negative bias exhibited by driving RCMs across the western Alps and the northern Apennines (5–20%). The driving RCM ensemble has a predominantly larger spread compared to the CPRCM's (Fig. S3, second row). The CPRCM ensemble tends to be positively biased with respect to observations, while the opposite is found for the RCMs (Table 2).

Along with the underestimation of the wet-day precipitation intensity, the 12 km RCM ensemble shows an overestimation of precipitation frequency (Fig. S1 and S2, third row), especially in JJA. This overestimation reflects the drizzle problem characteristic of most convection schemes and must be kept in mind when analyzing mean daily precipitation. In fact, while the mean precipitation from the 12 km RCM ensemble may look realistic, it may do so because of excessively frequent but too weak precipitation events. On the other hand, the CPRCM ensemble represents fairly well the observed frequency in JJA (Fig. 2, third row), while this improvement is less evident in SON (Fig. 3, third row), where the precipitation frequency remains mostly overestimated.

The two ensembles show similar uncertainty ranges in simulating wet event frequency in JJA (Fig. S3, third row, left panel), although the CPRCM ensemble is centered around the observed average over most areas, whereas most of the RCMs overestimate it. On the other hand, in SON (right panel) the two ensembles have comparable spreads except in some areas (e.g. IT and its sub-areas NIT/CIT/SIT, SFR) where the CPRCM ensemble shows lower uncertainty than the driving RCMs.

Finally, the 99th percentile of the daily precipitation is presented in Fig. S1 and S2 (fourth row). The results at the daily scale highlight improvements in line with findings at the hourly scale for both seasons, but it is worth emphasizing the ability of the CPRCM ensemble to produce heavy
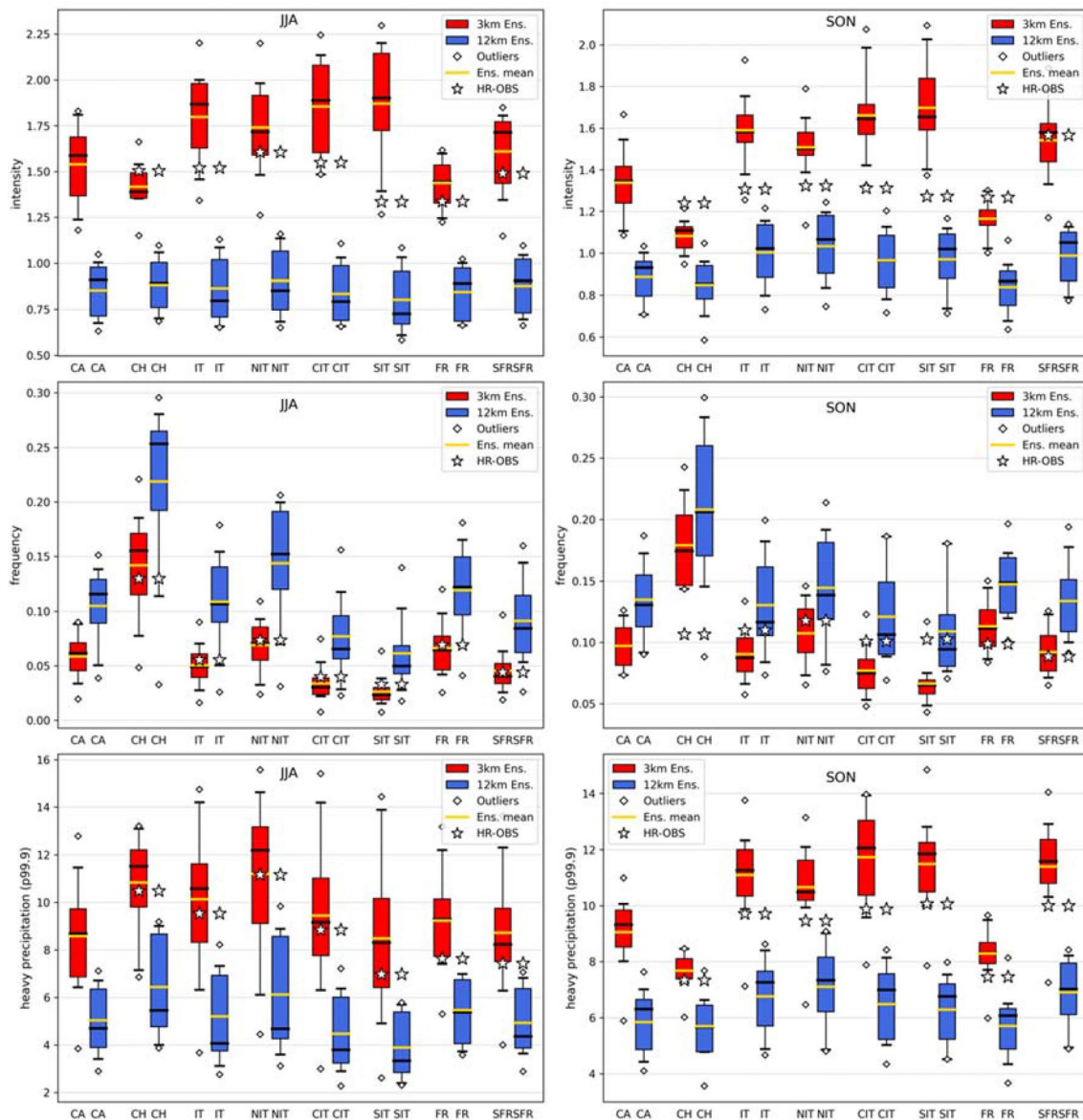
Fig. 4 JJA (left) and SON (right) box-plot representing the distribution of the CPRCM (red) and driving RCM (blue) ensemble members over different areas (CA: common domain as represented in Fig. 1, CH: Switzerland, (N/C/S)IT:(North/Central/South) Italy, (S) FR: (South) France) over the historical period 1996-2005. The distribution is represented within 5th and 95 percentile, for (from top to bottom) mean wet-hour intensity (mm/h), wet-hour frequency, heavy hourly precipitation (p99.9, mm/h). Outliers are represented singularly (open diamonds), ensemble mean (yellow line) is also reported and compared with the highest resolution observations (white star) over the same area (Sect. 3)

precipitation events during SON (Fig. S2, fourth row) in stark contrast to the 12 km RCM ensemble.

The ensemble spread of extreme precipitation events (Fig. S3, bottom row) is narrower for the CPRCMs within the first and third quartile, especially over complex terrain areas (CH, NIT), where the RCMs tend to give more uncertain results. It is also worth noting the large difference in extreme event intensity between high resolution (HR-OBS and EURO4M-APGD, SAFRAN) and low resolution observations (E_OBS).

Concerning the individual simulations in summer the WRF-BCCR model largely underestimates (outlier in the Fig. S3 distribution) and the RegCM-ICTP is on the lower end of the distribution for both the mean daily precipitation and the wet-day intensity, whereas AROME-CNRM, COSMO-ETH, CCLM-KIT and CCLM-WEG are at the far high end (overestimation) of the distribution over the Alps. The same behaviour is shown for the WRF-BCCR driving model, but not for the driving RegCM-ICTP. As these two members show a behaviour coherent with the rest of the

ensemble for the other seasons, we can speculate that they may have difficulty in initiating fine scale summer convection. Also, given the similar behavior in the driving RCM for WRF-BCCR, there may be further deficiencies in the land–atmosphere coupling or in soil forcings which can produce unrealistic lower boundary conditions, more evident during this strongly coupled season, and that need to be investigated in future. On the other hand, these models are able to better represent convection in seasons when other large scale forcings contribute to the convection phenomenology. Conversely, all CPRCMs showing an overestimation reflect the behaviour of their intermediate 12 km RCM, except the COSMO-ETH, which has a tendency to excessively trigger convection regardless of the boundary forcing.

5.1.3 Daily cycle evolution

The diurnal variation of precipitation is an important component of the climate of a region, and this is especially true in warm seasons across the Alpine area, where convection typically produces precipitation between the late afternoon and evening. The correct representation of the summer precipitation daily cycle is still an open issue in models, which

are often affected by an early onset of convection and an underestimation of precipitation intensity at sub-daily time scale (Ban et al. 2014, 2015; Brockhaus et al. 2008), mostly driven by the behavior of current convection parameterizations. The increase of resolution on one hand and the possibility of turning off the deep convection schemes on the other hand can thus lead to an improvement in the representation of the diurnal cycle through the CPRCMs (Prein et al. 2013).

Summer diurnal cycles of hourly precipitation indices (mean precipitation, wet-hour intensity, wet-hour frequency, 99th and 99.9th percentile precipitation) are shown in Figs. 5, 6 and 7, respectively, averaged over Switzerland, Italy and France. The plots report the cycles for the historical decade (dashed lines) to be compared with observations (black line) and for the end-of-century decade (solid lines), which will be discussed later. Each ensemble mean is reported with its standard deviation (diagonal shaded area for the 1996–2005 period). For some indices (intensity, heavy precipitation and also mean precipitation over some region) the RCMs (blue) reproduce poorly or not at all the observed evolution. By contrast, the CPRCM ensemble (dashed red line) increases the mean hourly precipitation
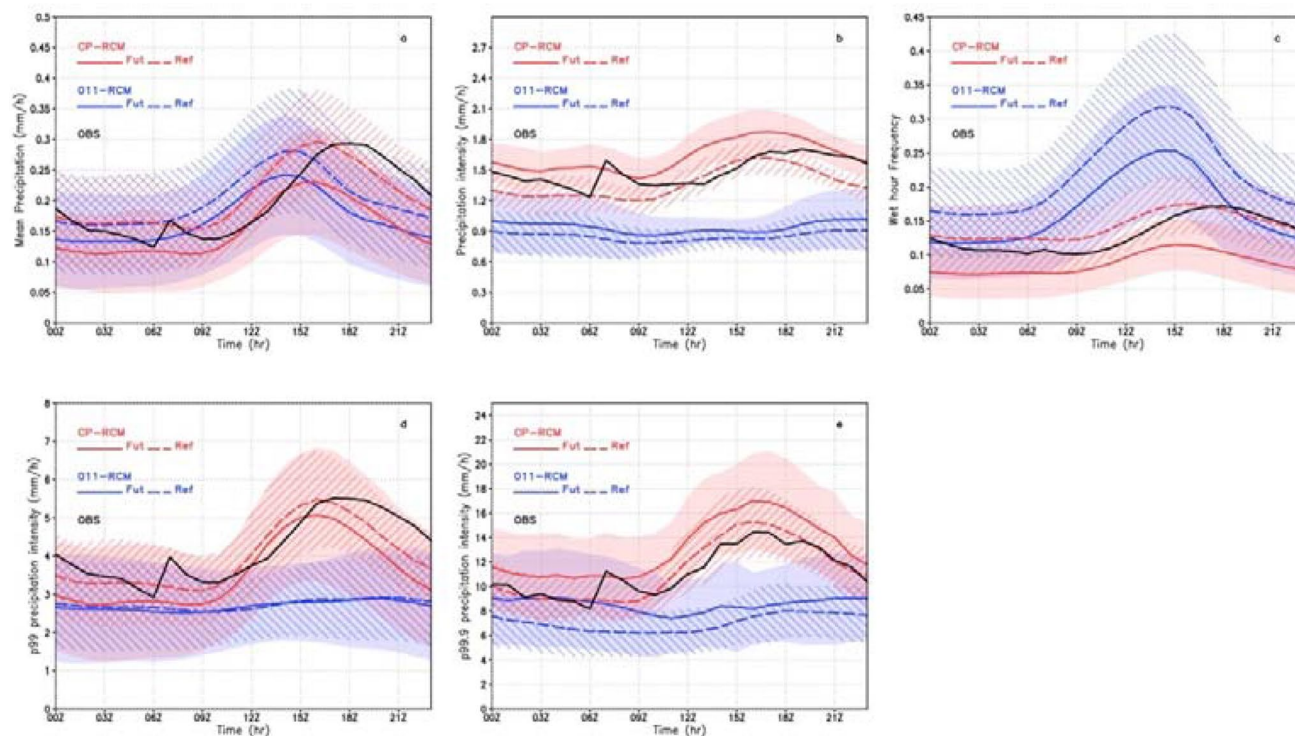

Fig. 5 Summer diurnal cycle of mean hourly precipitation (**a**, mm/h), hourly intensity precipitation (**b**, mm/h), wet-hour frequency (**c**), heavy hourly precipitation (p99 (**d**); p99.9 (**e**), mm/h) averaged over Switzerland. The black line reports the observations (black, Rdis-aggH dataset, Sect. 3); lines and corresponding shaded areas rep-resent the ensemble mean and standard deviation of the CPRCMs simulations (red) and of the corresponding driving RCMs simulations (blue) for the decade 2090–2099 (solid line and plain colour area) and for the reference period 1996–2005 (dashed line and diagonal lines area)
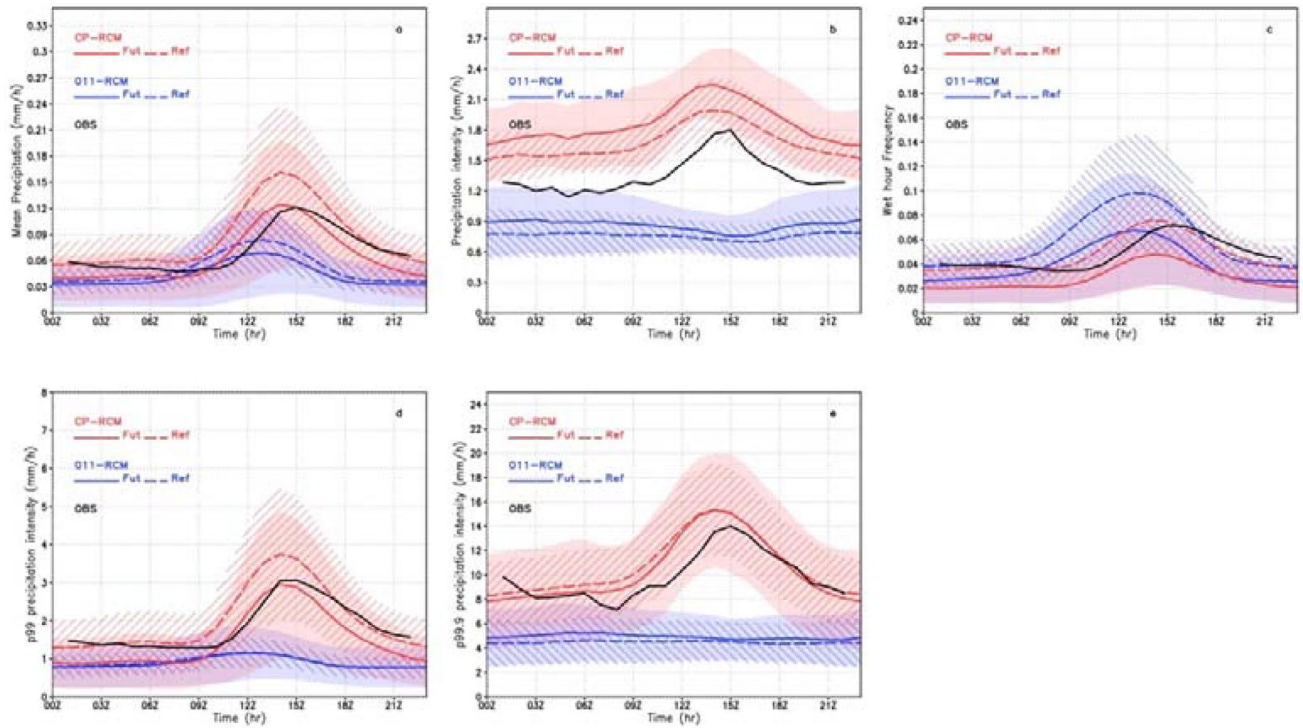
Fig. 6 As in Fig. 5 but averaged over Italy and with the observed GRIPHO data (black, Sect. 3)
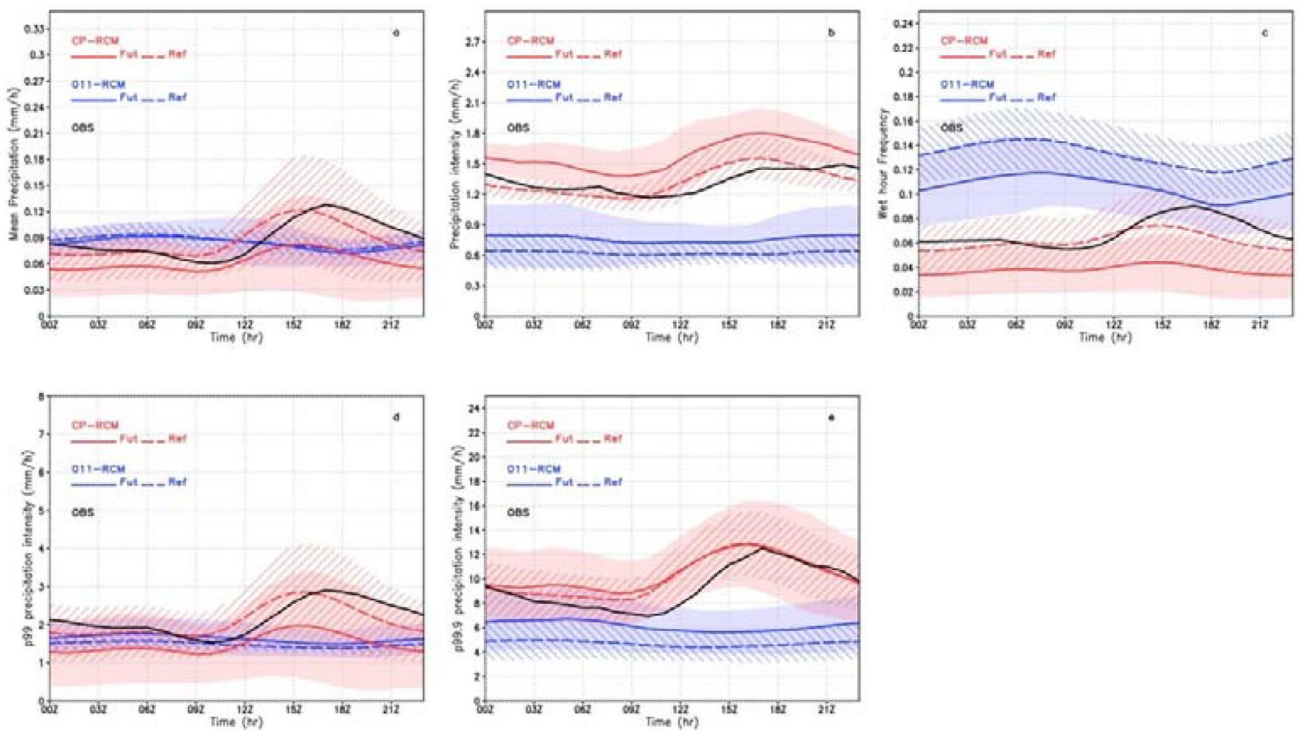

Fig. 7 As in Fig. 5 but averaged over France and with the observed COMEPHORE data (black, Sect. 3)

compared to the intermediate RCM ensemble (dashed blue line) regardless of the area considered, leading to a better comparison with observations (solid black line). The timing of the peak is also better reproduced by the CPRCM ensemble, which correctly delays the early onset of the diurnal precipitation peak found in the coarser resolution models, although still with an early timing bias compared to observations.

The diurnal maximum of convection/precipitation occurs in the late afternoon because of the strong relationship between convection and boundary layer heating (Wallace 1975; Dai et al. 1999), usually represented as sub-grid mechanisms in convection parameterization schemes. Other key factors, such as the moistening of the surrounding environment and convective inhibition (CIN) duration (Nesbitt and Zipser 2003) are poorly or not represented in cumulus schemes. The problem of early onset of convection (precipitation) in models is well known in GCMs (Lin et al. 2000; Bechtold et al. 2004) and it is related to the representation of convection triggering only through the diurnal evolution of convective available potential energy.

Brockhaus et al. (2008) demonstrated that an underestimation of both the CIN and the diurnal temperature range (leading to a shallower PBL) contribute to the early afternoon onset of the precipitation peak. The importance of such factors is well demonstrated by Rio et al. (2009), who conducted a single column model study showing that the preconditioning of sub-cloud processes through a stronger inhibition, along with a gradual moistening of the inversion layer, drive a more efficient switch from shallow to deep convection, thus contributing to an improved precipitation onset

and duration. Conversely, most schemes simulating convection in RCMs trigger convection only through the diurnal boundary layer heating. For the CPRCMs, direct errors coming from convection schemes are overcome by switching the deep convection schemes off. However, an early maximum is still observed (red dashed lines in Figs. 5, 6 and 7), for which errors affecting the PBL evolution and lower boundary conditions (e.g. soil moisture) can be important factors.

The improvement in the simulated diurnal cycle by the CPRCMs is quite evident for the wet-hour frequency (Figs. 5, 6 and 7, top row, right panels), as is the improvement in hourly precipitation intensity (Figs. 5, 6 and 7, top row, middle panels). The same is found for the heavy hourly precipitation diurnal cycle (Figs. 5, 6 and 7, bottom panels of p99 and p99.9): the CPRCM ensemble correctly increases the intensity of the heaviest events and better simulates their diurnal evolution, even though an early simulation of the maximum still persists.

5.1.4 Distribution of precipitation event intensity

The PDFs of hourly (daily) precipitation are shown in Fig. 8 (S4) over Italy (left), France (middle) and Switzerland (right). The plots report both the historical decade (black for observations, light blue and pink respectively for RCMs and CPRCMs) and the 2090–2099 one (blue and red respectively for RCMs and CPRCMs), which will be discussed later.

Referring to the historical period 1996–2005, the highest-resolution observed distributions (HR-OBS, black) show tails reaching between 90 and 200 mm/h (Fig. 8, depending on the area) for hourly precipitation (300–600 mm/day
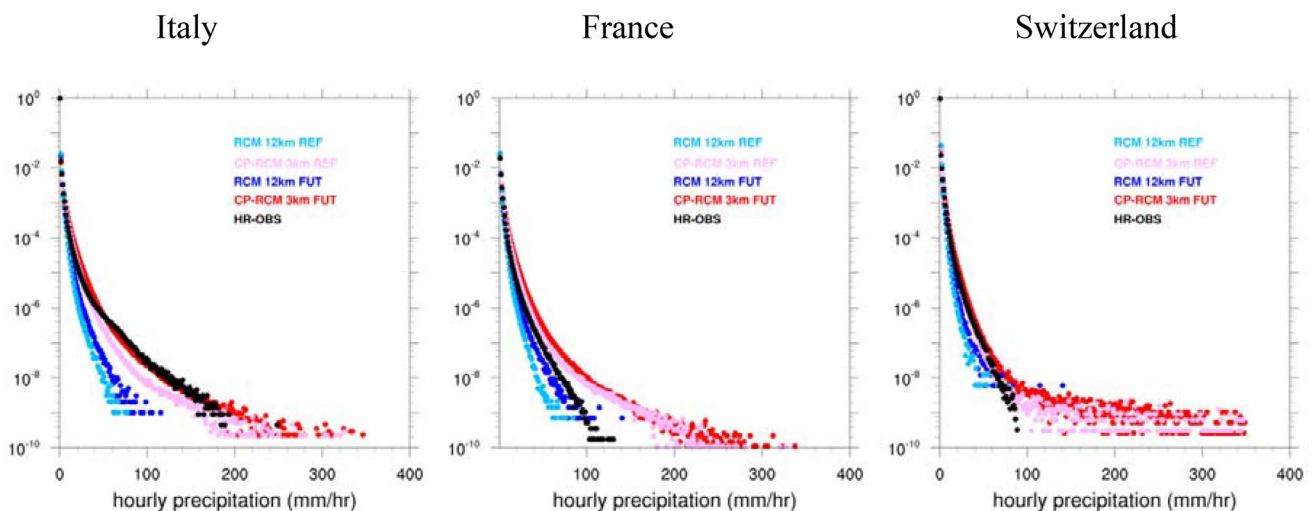

| Italy | France | Switzerland |

Fig. 8 Probability density function (PDF) of hourly precipitation (mm/h) over Italy (left), France (middle) and Switzerland (right) for the highest-resolution observed data over the historical decade (black, Sect. 3; GRIPHO for Italy, COMEPHORE for France, RdisaggH for Switzerland); for the CPRCM (pink for 1996–2005 and red for 2090–2099) and the driving RCM (light blue for 1996–2005 and blue for 2090–2099) ensembles

for daily precipitation, Fig. S4). The hourly precipitation PDFs (Fig. 8) show an underestimation by the coarse resolution ensemble (light blue), whereas the CPRCMs (pink) are closer to observations, but with a tendency to produce longer tails, i.e. an overestimation of the most extreme precipitation. In particular, over France (Fig. 8, middle) the CPRCM ensemble shows the greatest overestimation of the observed curve.

These biases in extreme precipitation can be due to different reasons: (1) large overestimations by a few ensemble members skewing the PDF of the ensemble; (2) the observed distribution might not fully represent the real tail of the precipitation distribution due to poor spatial coverage and/or undercatch (La Barbera et al. 2002); (3) occurrence of sporadic numerical point storms (Roberts 2003; Petch 2006). Moreover the GRIPHO dataset over Italy is generated from a non-uniform network with higher density of rain gauges in northern Italy than in the central and southern regions, and this can result in a skewed representation of the precipitation PDF there.

Similarly, the intermediate 12 km model ensemble (Fig. S4, light blue) underestimates daily precipitation distributions over Italy and France (left and middle panels), missing especially the extremes, while the CPRCMs are closer to observations, though again with a tendency to overestimate the most extreme events. Over Switzerland the CPRCMs (pink) tend to overestimate the observed distributions (both high and low resolution ones), whereas the RCMs (light blue) fall in between, although they miss the most extreme observed events (black).

Coarse resolution observations (E_OBS, EURO4M-APGD) and reanalysis (SAFRAN) are also reported for daily precipitation where available (Fig. S4). The pronounced differences among observed distributions highlight the uncertainty of the observed information especially for the most extreme precipitation events. It is evident that, as the model resolution increases, increasing resolution observations are needed for a more robust model assessment.

5.2 Assessment of end-of-century projected changes (2080–2099)

In this section we assess the changes in the precipitation characteristics at daily to hourly scales between the end-of-century and historical time slices. In this regard, note that the PGW approach adopted by ETH (ETHZb in Table 1) takes into account large scale dynamical changes (i.e. slow varying circulation changes) from a GCM but not fast circulation changes (Brogli et al. 2019). However, since the domain of the PGW simulation is large (covering almost the entire European region), there is sufficient space for the model to develop local circulation changes. As indicated by some previous studies, the differences between the PGW approach and the standard GCM-RCM nesting approach are not large (e.g. Ban et al. 2021; Liu et al. 2017; Prein et al. 2017b; Kröner et al. 2017; Brogli et al. 2019; Hentgen et al. 2019) and are smaller than the effect of using two different driving GCMs.

5.2.1 Summer projections

Future changes in summer hourly precipitation are shown in Fig. 9. An overall agreement between the two ensembles is found but with differences in magnitude mostly evident over topography. For most of the indices, the CPRCM ensemble shows a refinement of the spatial patterns of change and an intensification of the magnitudes of the changes in areas where the sign of the change is the same in the two ensembles.

The change in precipitation intensity is positive for both ensembles, though larger increases over the Alps and over open water occur in the CPRCM ensemble (Fig. 9, top row). The spread of the ensemble (Fig. 11, top left) is smaller for the CPRCMs than the RCMs across the whole domain (CA) and over most sub-regions. For some areas (SIT, SFR) the CPRCM members show agreement in sign in contrast to the 12 km models. Changes across some sub-regions are reported in Table 3.

The frequency changes are negative everywhere, with maxima over the mountains and greater in the CPRCM ensemble (Fig. 9, middle row). The signal is associated with a general smaller spread for the CPRCM ensemble (Fig. 11, middle left). This signal of more intense but less frequent events is consistent with previous analyses at regional to global scales (Giorgi et al. 2011, 2014, 2019).

Changes in heavy precipitation (Fig. 9, bottom row) show an increase of intensity of extreme events in the northern part of the domain for the RCMs (right) and a decrease southward. The CPRCM ensemble (left) maintains the same sign of the signal over most of the domain, but exhibits a greater spatial correlation with topography and places the largest changes over the Alps and western Mediterranean, with modest increases elsewhere. The negative change signal is more extended northward in the CPRCMs, thus resulting in a switch of sign compared to the RCMs over part of northern Italy (subalpine region) and central-northern France. A larger spread is found for the CPRCMs than the RCMs over many of the sub-regions (Fig. 11, bottom left), although there is a greater agreement in sign among the ensemble members over the whole domain (CA) and some sub-regions (CIT, SIT and SFR).

Results at the daily scale are available in figure S5. Summer mean daily precipitation (Fig. S5, top row) decreases across the entire domain at both resolutions, with slightly lower drying at high altitudes, a result consistent for example with Giorgi et al. (2016). Results for wet-indices at the daily
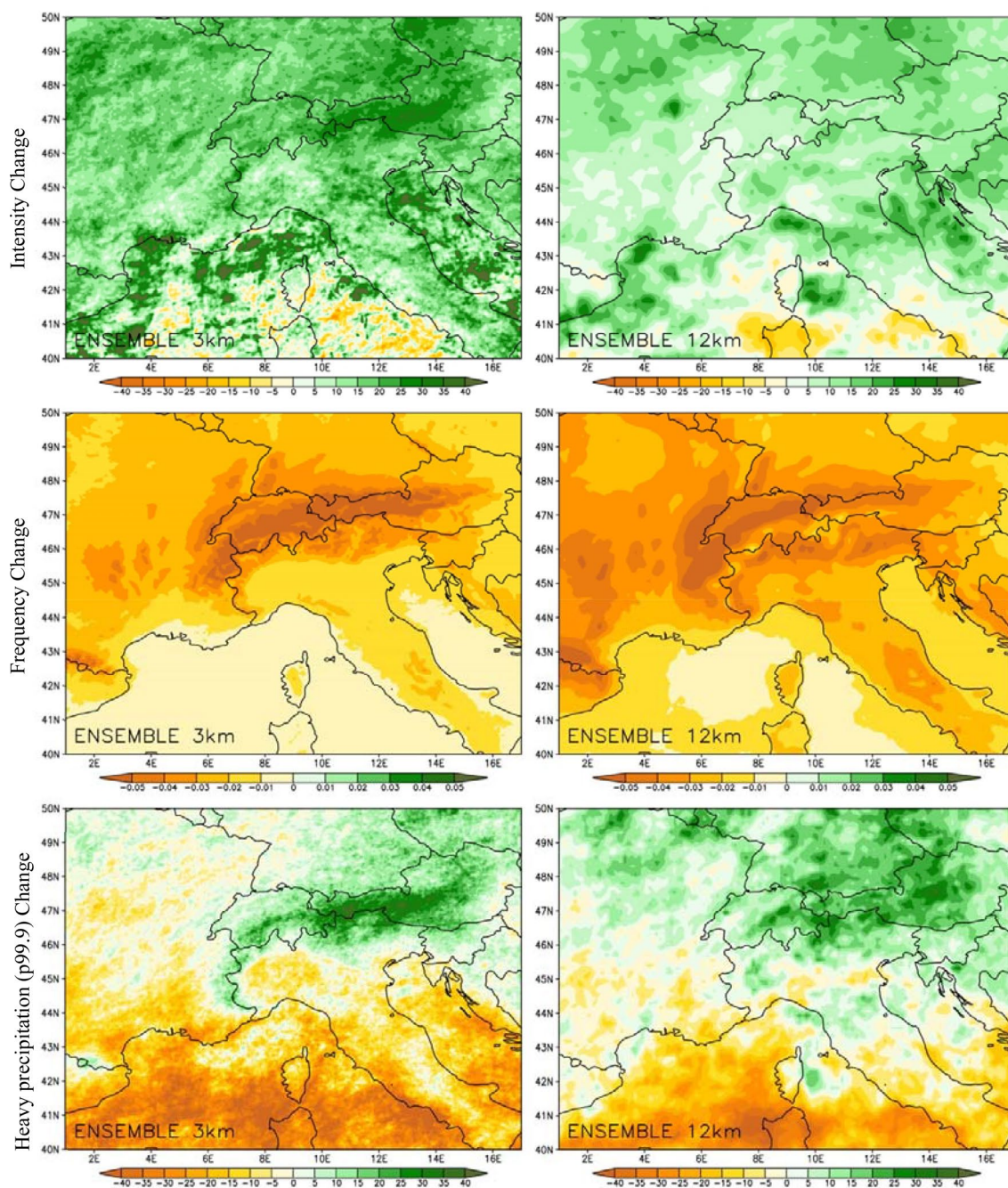
Fig. 9 Ensemble mean percent change of the indices analysed over 2090–2099 for the summer hourly precipitation (historical simulation is the reference, 1996–2005). From top to bottom: intensity, frequency (change) and heavy precipitation (p99.9). The results are obtained from the CPRCM ensemble (left) and the driving RCM ensemble (right)

scale reflect the hourly scale response. The precipitation frequency decreases (Fig. S5, third row), while heavy precipitation is intensified over the eastern Alps and the northern part of the domain, and decreases over the southern part (Fig. S5, fourth row).

The most important difference between the two ensembles is found for the changes in precipitation intensity,

which are positive over almost all areas of the domain in the CPRCMs, while the RCM ensemble suggests a decrease over the western Alps and northern Apennines (Fig. S5, second row). This pattern indicates a sign change in the precipitation intensity response when moving to convection permitting scales. Assessing the robustness and reasons of this

Table 3 Changes (FREQ) and percentage changes (other indices) as given by the two ensembles (3 km CPRCMs and 12 km RCMs) for analysed indices averaged over sub-areas (as in Fig. 1, CH: Switzerland, (N/C/S)IT:(North/Central/South) Italy, (S)FR: (South) France) for JJA and SON over the end-of century 2090–2099

2090–99	CH		IT		NIT		CIT		SIT		FR		SFR	
	3 km	12 km	3 km	12 km	3 km	12 km	3 km	12 km	3 km	12 km	3 km	12 km	3 km	12 km
JJA														
Mean PR-d	− 29.98	− 15.86	− 36.27	− 28.45	− 29.38	− 20.49	− 33.20	− 29.99	− 46.28	− 33.36	− 34.68	− 25.52	− 39.25	− 32.59
INT-d	2.99	1.39	5.21	2.55	5.79	4.36	9.12	9.80	4.36	2.64	7.28	5.12	5.10	1.025
FREQ-d	− 0.11	− 0.06	− 0.05	− 0.06	− 0.07	− 0.06	− 0.05	− 0.05	− 0.04	− 0.03	− 0.09	− 0.08	− 0.06	− 0.07
P99-d	− 6.21	1.65	− 24.51	− 14.94	− 11.96	− 4.02	− 22.33	− 12.22	− 42.73	− 27.55	− 12.75	− 4.74	− 24.06	− 17.66
INT-h	20.86	9.08	15.37	7.59	18.27	10.85	17.21	12.52	11.59	7.04	17.88	10.92	15.42	7.40
FREQ-h	− 0.05	− 0.05	− 0.02	− 0.03	− 0.02	− 0.04	− 0.01	− 0.02	− 0.01	− 0.01	− 0.03	− 0.04	− 0.02	− 0.03
P99.9-h	13.41	14.78	− 14.49	− 4.81	1.56	6.60	− 13.63	− 2.73	− 35.66	− 20.40	− 4.80	1.90	− 13.15	− 7.09
SON														
Mean PR-d	− 3.59	1.60	− 9.63	− 4.63	− 14.51	− 5.89	− 5.95	− 1.78	− 5.63	− 5.74	− 4.07	− 1.55	− 13.48	− 9.16
INT-d	9.73	9.18	16.98	10.65	12.88	10.29	19.44	13.23	21.11	13.60	15.32	11.4	13.37	9.84
FREQ-d	− 0.04	− 0.02	− 0.04	− 0.03	− 0.05	− 0.03	− 0.04	− 0.03	− 0.04	− 0.03	− 0.04	− 0.03	− 0.05	− 0.04
P99-d	8.15	8.81	8.26	9.12	3.96	9.03	10.87	12.37	11.79	4.06	11.06	10.57	2.31	6.58
INT-h	17.14	12.67	24.29	13.86	22.93	14.97	24.99	14.49	25.48	18.26	21.84	14.66	21.18	13.55
FREQ-h	− 0.03	− 0.02	− 0.02	− 0.02	− 0.03	− 0.02	− 0.02	− 0.01	− 0.01	− 0.01	− 0.02	− 0.02	− 0.02	− 0.02
P99.9-h	23.35	21.46	20.75	16.44	22.06	19.64	21.61	16.29	18.27	12.98	22.64	17.60	16.33	13.36

Flag "d" and "h" refer to daily and hourly indices

switch in sign requires a more in depth and physically-based analysis to be carried out in future work.

Mean precipitation and frequency changes show agreement in sign among most members of the two ensembles (Fig. S7, left column). This is still true over most sub-regions for the CPRCMs when considering changes in daily intensity. Overall for these indices, the CPRCM ensemble shows a reduced spread than driving RCMs over most sub-regions. In terms of extreme precipitation (p99) the CPRCMs reduce the spread in the change signal only over some sub-regions (IT, NIT, SIT) and show a greater consistency in sign over some areas (NIT, FR) than the corresponding RCMs.

5.2.2 Autumn projections

Similarly to summer, the climate change signal for indices at the hourly scale is consistent between the CPRCM and RCM ensembles in autumn (Fig. 10). The precipitation intensity changes are positive everywhere but are much stronger in the CPRCM ensemble, particularly over the Adriatic and the Po river valley (Fig. 10, top row). The frequency changes are negative almost everywhere with stronger decreases over high topography in the CPRCM ensemble and lowered values with respect to RCM ensemble over the western Mediterranean (Fig. 10, middle row). Unlike summer, the fall exhibits strong increases in heavy precipitation over the entire domain (Fig. 10, bottom row). The CPRCMs show a similar or greater uncertainty than the RCMs for intensity (Fig. 11, top right) but a predominantly smaller spread for p99.9 (Fig. 11, bottom right).

The daily mean precipitation changes in fall (Fig. S6, top row) at both resolutions show a North–South dipole pattern (increase in the north, decrease in the south) in line with available literature (Giorgi and Coppola 2007; Kovats et al. 2014; Jacob et al. 2018; Coppola et al. 2020b). Except for the CPRCMs over some areas (NIT, SFR), the sign of the change is not uniform across any of the two ensembles (Fig. S7, top right) and a larger uncertainty occurs for the CPRCMs, due to differences among models in representing the spatial extension of positive/negative pattern and by some models producing different patterns. The intensity changes are positive nearly everywhere and coherent between the two ensembles, with a slight increase in magnitude in the CPRCMs over the eastern part of the domain (Fig. S6, second row) and comparable large uncertainties (Fig. S7, second row right). The changes in frequency are more uniform in fall than in summer and indicate a decrease nearly everywhere, with stronger decreases over mountain areas (Fig. S6, third row) and a generally larger spread for the CPRCMs than the RCMs (Fig. S7, third row left). Heavy precipitation is enhanced nearly everywhere at both resolutions except over the Swiss Alps, Northern Apennines and Southwest Mediterranean (Fig. S6, fourth row), with

comparable spread between the two ensembles (Fig. S7, bottom right).

5.2.3 Diurnal cycle and precipitation event distributions

Figures 5, 6 and 7 show the summer diurnal cycles for different indices over the Switzerland, Italy and France subregions. Hourly means are compared for both the CPRCM (red lines) and driving RCM (blue lines) ensembles between the future decade (solid lines) and the historical period (dashed lines).

The two ensembles show coherent decreasing signals of mean hourly precipitation (panels a) and wet-hour frequency (panels c) and increases of precipitation intensity (panels b). The changes are larger for the CPRCMs than for the driving RCMs, and especially around the diurnal peaks. This is also shown for the decrease of p99 (panels d), which in France also represents a switch in sign between CPRCMs and RCMs (Fig. 7d). Moreover, the CPRCMs show smoother gradients in the damping phase of the diurnal peak, especially for mean precipitation and p99 over Italy and France, suggesting a slightly longer duration of convection.

A more pronounced change for some indices (mainly over France and Italy) across the peak of the diurnal cycle suggests that some local mechanisms or complex mesoscale interactions may play a major role and make some differences on the response of diurnal evolution of convection to climate change over areas characterized by different prevailing mesoscale interactions (orographic, complex sea-land interactions typical of the Mediterranean area, continental with influence of the Atlantic). Standard deviations of each ensemble are also plotted (plain color shaded area for end-of-century decade and diagonal lines areas for historical period curves), illustrating the ensemble's deviation from the mean, which is found to be generally larger for the CPRCMs than for the RCMs.

Finally, the PDFs in blue and red in Fig. 8 (S4) show changes of hourly (daily) precipitation distribution of each ensemble. Both ensembles show positive change of heavy hourly precipitation over all regions (Fig. 8), thus revealing an increase in their frequency, even with a decrease in the total number of events (e.g. Giorgi et al. 2019). Over Switzerland, where orographic forcings prevail, the two ensembles tend to produce similar changes, whereas the CPRCMs produce larger increases than RCMs over Italy, smaller over France. Anyway the CPRCMs allow to highlight differences in changes between heavy and extreme hourly events, which are not possible to inspect by RCMs due to their shorter tails. Indeed, from CPRCMs it is found that changes, mainly over Italy, are more pronounced for very heavy to severe precipitation (50–150 mm/h) than for the most extreme events at the very end of the tail. At the daily scale (Fig. S4) the two
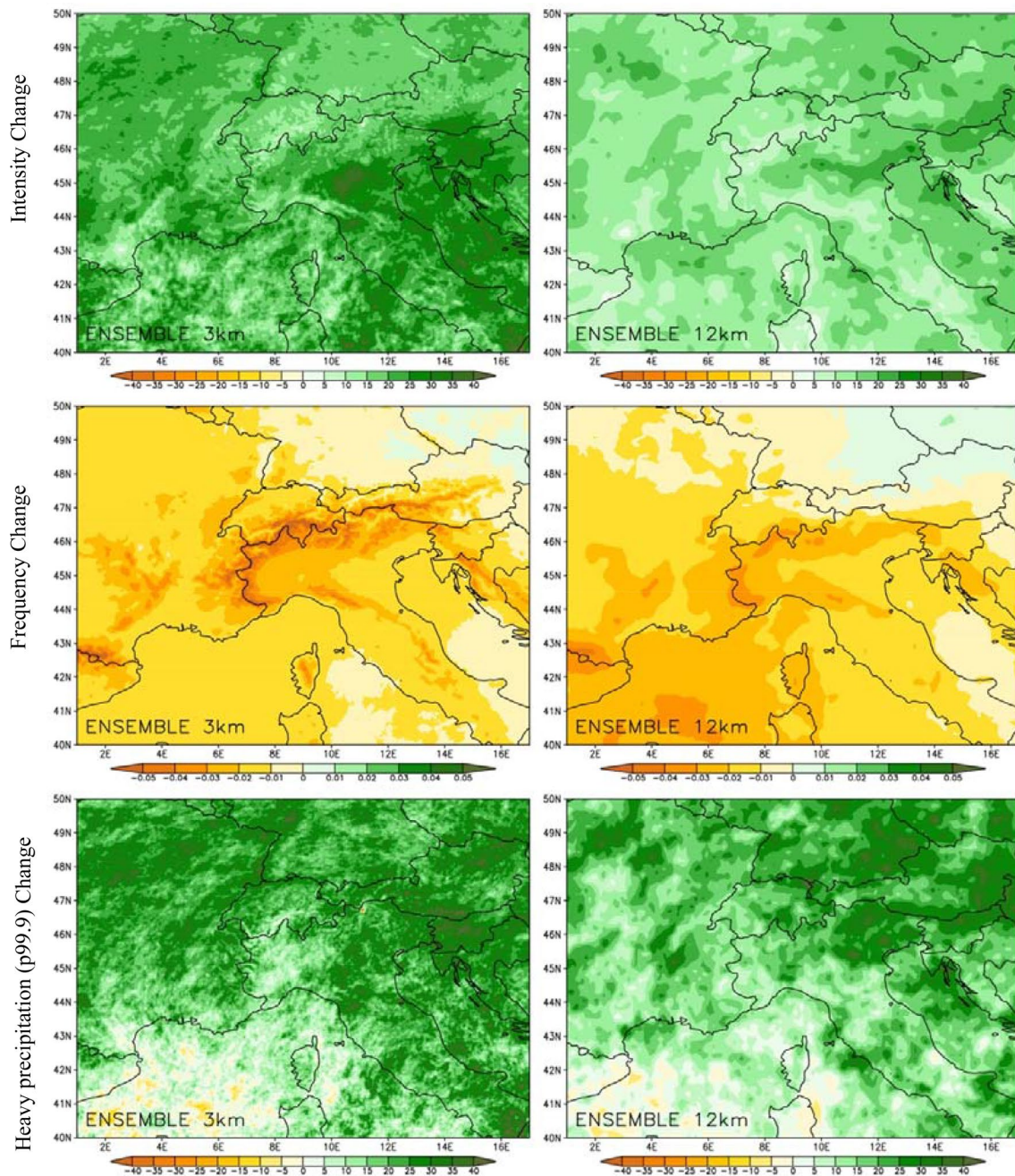
Fig. 10 Same as Fig. 9 but for autumn hourly precipitation mean change

ensembles show similar tendencies, but with larger increases in CPRCMs only over Italy.

6 Conclusions

In this study we analyze a multi-model ensemble of km-scale climate simulations of present and projected precipitation over a greater Alpine domain. The simulations are driven by intermediate resolution RCMs (~12 km grid spacing), themselves driven by CMIP5 GCMs. Along with two companion papers (Ban et al. 2021, and Coppola et al. 2020a), this represents one of the first efforts to construct such an ensemble at convection permitting scales. The benefits of going to such high resolution are clear if one is interested in assessing changes at local to regional scales and/or in investigating extreme precipitation processes (e.g., Prein et al. 2015). Previous climate change experiments at these resolutions have been carried out
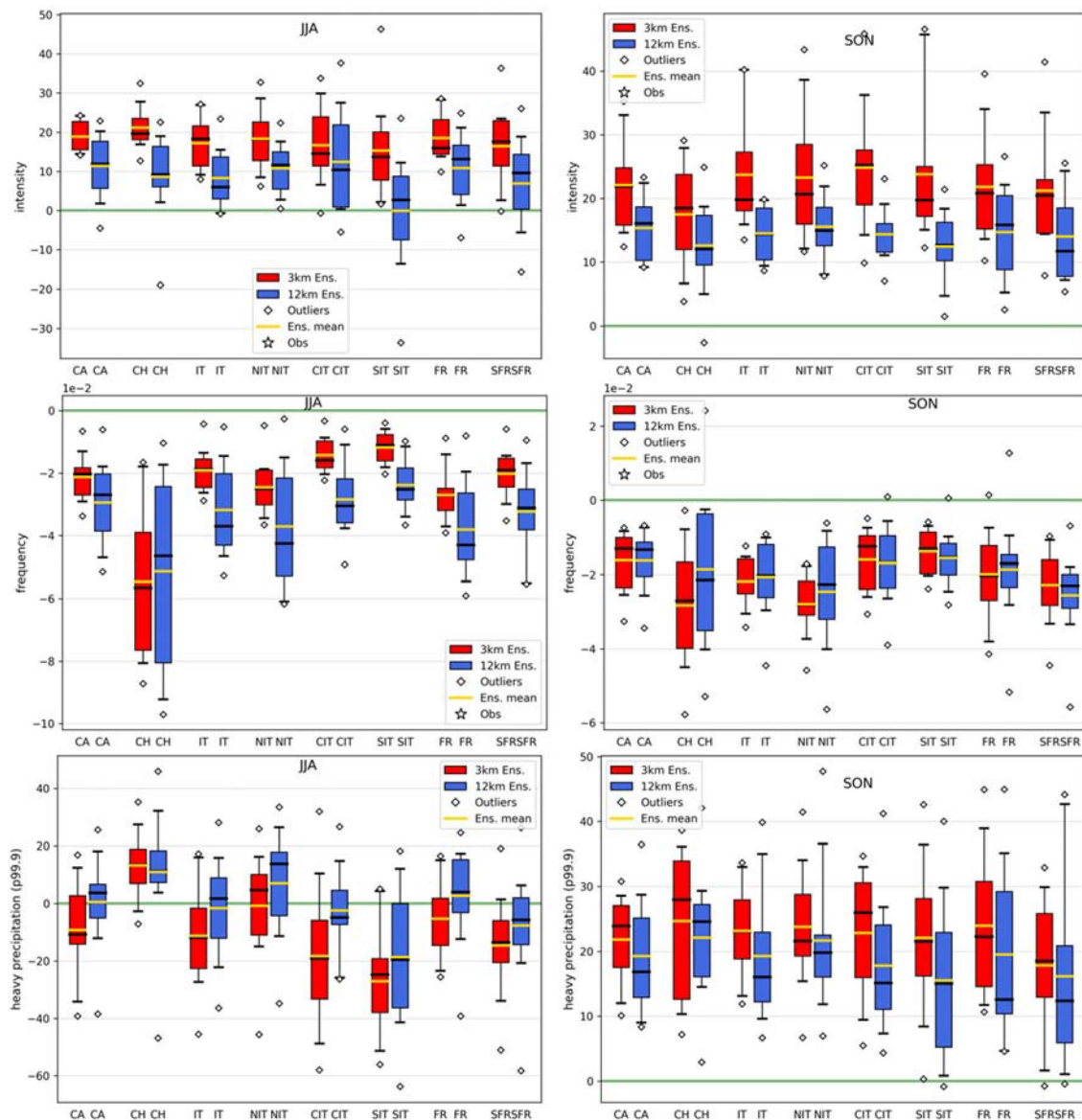
Fig. 11 JJA (left) and SON (right) box-plot representing the distribution of the percent change signal within the population of the CPRCM (red) and driving RCM (blue) ensembles over different areas (CA: common domain area as in Fig. 1, CH: Switzerland, (N/C/S) IT:(North/Central/South) Italy, (S)FR: (South) France) over 2090-99.

The distribution is represented within the 5th and 95 percentile, for (from top to bottom) mean wet-hour intensity, wet-hour frequency, heavy hourly precipitation (p99.9). Outliers are represented singularly (open diamonds); the zero is plotted in green

with single models, which places limits on their robustness (e.g., Kendon et al. 2019).

We compare results from the CPRCM and the driving RCM ensembles in 10-year long present day (1996–2005) and end-of-century (2090–2099) simulations (RCP8.5 scenario). Apart from the resolution, the main difference between the two ensembles is the treatment of deep convective processes, which are explicitly resolved by the CPRCMs, while are parameterized through cumulus convection schemes in the driving 12 km models. The experiments were conducted as part of the CORDEX-FPS

initiative (Coppola et al. 2020a) and the European EUCP project.

The ensemble performance for the historical period is assessed against various high resolution observation datasets, confirming findings from Ban. et al. (accepted), which highlights both the added value of the CPRCM simulations with respect to the coarser resolution RCMs and the value of the multi-model ensemble approach. Such added value mainly derives from a better representation of fine scale details of the precipitation patterns and a reduction of biases with respect to observations for most of the statistical indices

analyzed (mean daily precipitation, wet-day/hour frequency, wet-day/hour intensity and heavy precipitation events). In particular, the km-scale simulations largely improve the so-called "drizzle problem" in the coarser resolution models, i.e. the tendency to trigger excessively frequent and weak precipitation events. An improved representation of both precipitation frequency and intensity at the hourly scale, also yields corresponding improvements at the daily scale. The CPRCM ensemble also shows a considerable improvement of the precipitation diurnal cycle, as found in previous studies (e.g. Prein et al. 2015), in terms of timing, by shortening the early onset of diurnal convection as seen in RCMs, of intensity and of hourly extremes representation.

The spread of CPRCM ensemble is generally lower than for the RCMs in SON and over some regions, such as Southern France and Northern Italy, that are greatly exposed to high impact weather during this season.

The results for the future projections show that the two ensembles are mostly in agreement, but with larger changes by the CPRCMs. On the other hand a sign change between the 3 km and the 12 km models is found over some areas for hourly heavy precipitation and daily intensity in summer.

The summer mean precipitation is projected to be predominantly reduced across the greater alpine region, mostly because of a reduction in the frequency of rainfall events. Summer extreme precipitation is likely to decrease over the southern part of the domain. In autumn, the mean precipitation shows a North/South increase/decrease dipole in the precipitation change signal, but with a pronounced uncertainty across the ensemble related to the different representation of the spatial extension of this signal among most models and by some models producing different patterns. The frequency of precipitation is projected to decrease across most of the domain, while the intensity increases, with heavy precipitation becoming more intense at both the hourly and daily time scales. This new generation of convection-permitting models exacerbates these change signals, showing a reduced uncertainty compared to the RCMs for most indices and over most of the analyzed areas, and especially noteworthy for heavy precipitation in fall season. Moreover, confirming an increase in frequency of heavy precipitation in a context of decreasing total number of events, the CPRCMs highlight for some regions that this increase is more pronounced for heavy to severe events than for the most extreme ones.

The sign change of heavy precipitation is also evident on the diurnal evolution over France and Italy. The temporal evolution of the indices also shows that the greatest changes produced by the CPRCM ensemble occur around the diurnal peak of convection on some area, suggesting the possibility that some local mechanisms/interactions may have a greater role in the response of the diurnal convection to the climate change. At the same time a smoother damping of the peak suggests a longer duration of the diurnal convection over some areas.

Here we presented a first analysis of this multi-model CPRCM simulation ensemble; although further studies are required to confirm that the modifications shown by this ensemble are physically plausible and indeed improve the projection of precipitation changes, previous studies suggest that this may well be the case (Torma et al. 2015; Giorgi et al. 2016; Kendon et al. 2017; Prein et al. 2017a). Also, physically-based analyses linking precipitation in convection permitting models to driving physical processes could prove illuminating in this regard (e.g., Poujol et al. 2019). We might therefore expect to see more examples of this behavior as the model resolution reaches the km scale, with profound implications for the impacts of future changes in precipitation characteristics.

References

Baldauf M, Seifert A, Foerstner J, Majewski D, Raschendorfer M, Reinhardt T (2011) Operational convective-scale numerical weather prediction with the COSMO model: description and sensitivities. Mon Weather Rev 139:3887–3905. https://doi.org/10.1175/MWR-D-10-05013.1

Ban N, Schmidli J, Schär C (2014) Evaluation of the convection-resolving regional climate modeling approach in decade-long simulations. J Geophys Res Atmos 119:7889–7907. https://doi.org/10.1002/2014JD021478

Ban N, Schmidli J, Schär C (2015) Heavy precipitation in a changing climate: does short-term summer precipitation increase faster? Geophys Res Lett 42:1165–1172. https://doi.org/10.1002/2014GL062588

Ban N, Brisson E, Caillaud C, Coppola E, Pichelli E, Sobolowski S et al (2021) The first multi-model ensemble of regional climate simulations at the kilometer-scale resolution, Part I: Evaluation of precipitation. Clim Dyn (accepted)

Bechtold P, Chaboureau J-P, Beljaars A, Betts AK, Kohler M, Miller M, Redelsperger J-L (2004) The simulation of the diurnal cycle of convective precipitation over land in a global model. Q J R Meteorol Soc 130:3119–3137

Belušić D, de Vries H, Dobler A, Landgren O, Lind P, Lindstedt D, Pedersen RA, Sánchez-Perrino JC, Toivonen E, van Ulft B, Wang F, Andrae U, Batrak Y, Kjellström E, Lenderink G, Nikulin G, Pietikäinen J-P, Rodríguez-Camino E, Samuelsson P, van Meijgaard E, Wu M (2020) HCLIM38: a flexible regional climate model applicable for different climate zones from coarse to convection-permitting scales. Geosci Model Dev 13:1311–1333. https://doi.org/10.5194/gmd-13-1311-2020

Berthou S, Kendon E, Chan S, Ban N, Leutwyler D, Schar C, Fosser G (2018) Pan-European climate at convection-permitting scale: a model intercomparison study. Clim Dyn. https://doi.org/10.1007/s00382-018-4114-6

Brockhaus P, Lüthi D, Schär C (2008) Aspects of the diurnal cycle in a regional climate model. Meteorol Z 17:433–443

Brogli R, Kröner N, Sørland SL, Lüthi D, Schär C (2019) The role of Hadley circulation and lapse-rate changes for the futureEuropean summer climateJ. Climate 32:385–404

Caillaud C, Somot S, Alias A, Bernard-Bouissières I, Fumière Q, Laurantin O, Seity Y, Ducrocq V (2020) Modelling Mediterranean Heavy Precipitation Events at climate scale: an object-oriented evaluation of the CNRM-AROME Convection-Permitting Regional Climate Model. Clim Dyn. https://doi.org/10.1007/s00382-020-05558-y

Chan SC, Kendon EJ, Fowler HJ, Blenkinsop S, Ferro CAT, Stephenson DB (2013) Does increasing the spatial resolution of a regional climate model improve the simulated daily precipitation? Clim Dyn 41(5):1475–1495. https://doi.org/10.1007/s00382-012-1568-9

Chan SC, Kendon EJ, Roberts NM, Fowler HJ, Blenkinsop S (2016) Downturn in scaling of UK extreme rainfall with temperature for future hottest days. Nat Geosci 9:24–28

Chan SC, Kendon EJ, Berthou S et al (2020) Europe-wide precipitation projections at convection permitting scale with the Unified Model. Clim Dyn 55:409–428. https://doi.org/10.1007/s00382-020-05192-8

Coppola E, Sobolowski S, Pichelli E et al (2020a) A first-of-its-kind multi-model convection permitting ensemble for investigating convective phenomena over Europe and the Mediterranean. Clim Dyn 55:3–34. https://doi.org/10.1007/s00382-018-4521-8

Coppola E, Nogherotto R, Ciarlo JM, Giorgi F, van Meijgaardm E, Iles C et al (2020b) Assessment of the European climate projections as simulated by the large EURO-CORDEX regional climate model ensemble. J Geophys Res Atmos. https://doi.org/10.1029/2019JD032356

Cornes R, van der Schrier G, van den Besselaar EJM, Jones PD (2018) An ensemble version of the E-OBS temperature and precipitation datasets. J Geophys Res Atmos. https://doi.org/10.1029/2017JD028200

Dai A, Giorgi F, Trenberth KE (1999) Observed and model-simulated diurnal cycles of precipitation over the contiguous United States. J Geophys Res 104(D6):6377–6402

Dirmeyer PA et al (2012) Simulating the diurnal cycle of rainfall in global climate models: resolution versus parametrization. Clim Dyn 39:399–418

Ducrocq V, Braud I, Davolio S, Ferretti R, Flamant C, Jansa A, Kalthoff N, Richard E, Taupier-Letage I, Ayral PA, Belamari S, Berne A, Borga M, Boudevillain B, Bock O, Boichard JL, Bouin MN, Bousquet O, Bouvier C, Chiggiato J, Cimini D, Corsmeier U, Coppola L, Cocquerez P, Defer E, Drobinski P, Dufournet Y, Fourrie N, Gourley JJ, Labatut L, Lambert D, Le Coz J, Marzano FS, Molinie G, Montani A, Nord G, Nuret M, Ramage K, Rison B, Roussot O, Said F, Schwarzenboeck A, Testor P, Van Baelen J, Vincendon B, Aran M, Tamayo J (2014) HyMeX-SOP1, the field campaign dedicated to heavy precipitation and flash flooding in the northwestern Mediterranean. Bull Am Meteorol Soc 95:1083–1100. https://doi.org/10.1175/BAMS-D-12-00244

Fantini A (2019) Ph. D. Thesis: climate change impact on flood hazard over Italy. http://hdl.handle.net/11368/2940009

Fosser G, Khodayar S, Berg P (2015) Benefit of convection permitting climate model simulations in the representation of convective precipitation. Clim Dyn 44:45–60. https://doi.org/10.1007/s00382-014-2242-1

Fosser G, Khodayar S, Berg P (2017) 2016: climate change in the next 30 years: what can a convection-permitting model tell us that we did not already know? Clim Dyn 48:1987. https://doi.org/10.1007/s00382-016-3186-4

Fosser G, Kendon E, Chan S, Lock A, Roberts N, Bush M (2019) Optimal configuration and resolution for the first convection-permitting ensemble of climate projections over the United Kingdom. Int J Climatol. https://doi.org/10.1002/joc.6415

Fumière Q, Déqué M, Nuissier O, Somot S, Alias A, Caillaud C, Laurantin O, Seity Y (2019) Extreme rainfall in Mediterranean France during the fall: added-value of the CNRM-AROME Convection-Permitting Regional Climate Model. Clim Dyn. https://doi.org/10.1007/s00382-019-04898-8)

Giorgi F (2019) Thirty years of regional climate modeling: where are we and where are we going next? J Geophys Res Atmos 124:5696–5723. https://doi.org/10.1029/2018JD030094

Giorgi F, Im E-S, Coppola E, Diffenbaugh NS, Gao XJ et al (2011) Higher hydroclimatic intensity with global warming. J Clim 24:5309–5324

Giorgi F, Coppola E, Solmon F, Mariotti L et al (2012) RegCM4: model description and preliminary tests over multiple CORDEX domains. Clim Res 52:7–29. https://doi.org/10.3354/cr01018

Giorgi F, Coppola E, Raffaele F, Diro GT, Fuentes-Franco R et al (2014) Changes in extremes and hydroclimatic regimes in the CREMA ensemble projections. Clim Change 125:39–51

Giorgi F, Torma C, Coppola E, Ban N, Schär C, Somot S (2016) Enhanced summer convective rainfall at Alpine high elevations in response to climate warming. Nat Geosci 9(8):584–589. https://doi.org/10.1038/ngeo2761

Giorgi F, Raffaele F, Coppola E (2019) The response of precipitation characteristics to global warming from climate projections. Earth Syst Dyn 10:73–89

Gleckler PJ, Taylor KE, Doutriaux C (2008) Performance metrics for climate models. J Geophys Res 113(D6):D06104. https://doi.org/10.1029/2007JD008972

Hentgen L, Ban N, Kröner N, Leutwyler D, Schär C (2019) Clouds in convection-resolving climate simulations over Europe. J Geophys Res Atmos 124:3849–3870. https://doi.org/10.1029/2018JD030150

Herold N, Alexander L, Donat M, Contractor S, Becker A (2015) How much does it rain over land? Geophys Res Lett 43:341–348. https://doi.org/10.1002/2015GL066615

Herrera S, Gutierrez JM, Ancell R, Pons MR, Frias MD, Fernandez J (2010) Development and Analysis of a 50 year high-resolution daily gridded precipitation dataset over Spain (Spain02). Int J Climatol. https://doi.org/10.1002/joc.2256 **(In press)**

Isotta F, Frei C, Weilguni V, Tadić MP, Lassegues P, Rudolf B, Pavan V, Cacciamani C, Antolini G, Ratto SM, Munari M, Micheletti S, Bonati V, Lussana C, Ronchi C, Panettieri E, Marigo G, Vertacnik G (2014) The climate of daily precipitation in the Alps: development and analysis of a high-resolution grid dataset from pan-Alpine rain-gauge data. Int J Climatol 34(5):1657–1675. https://doi.org/10.1002/joc.3794

Isotta FA, Vogel R, Frei C (2015) Evaluation of European regional reanalyses and downscalings for precipitation in the Alpine region. Meteorol Z 24:15–37. https://doi.org/10.1127/metz/2014/0584

Jacob D, Petersen J, Eggert B, Alias A, Christensen OB, Bouwer LM et al (2014) EURO-CORDEX: new high-resolution climate change projections for European impact research. Reg Environ Change 14(2):563–578. https://doi.org/10.1007/s10113-013-0499-2

Jacob D, Kotova L, Teichmann C, Sobolowski SP, Vautard R, Donnelly C, Koutroulis AG, Grillakis MG, Tsanis IK, Damm A, Sakalli A, van Vliet MTH (2018) Climate impacts in Europe under +1.5 C global warming. Earth's Future 6:264–285. https://doi.org/10.1002/2017EF000710

Jacob D, Teichmann C, Sobolowski S et al (2020) Regional climate downscaling over Europe: perspectives from the EURO-CORDEX community. Reg Environ Change 20:51. https://doi.org/10.1007/s10113-020-01606-9

Kendon EJ et al (2019) UKCP Convection-permitting model projections: science report. UK Met Office

Kendon EJ, Roberts NM, Senior CA, Roberts MJ (2012) Realism of rainfall in a very high resolution regional climate model. J. Clim 25:5791–5806. https://doi.org/10.1175/JCLI-D-11-00562.1

Kendon EJ, Ban N, Roberts NM, Fowler HJ, Roberts MJ, Chan SC et al (2017) Do convection-permitting regional climate models improve projections of future precipitation change? Bull Am Meteor Soc 98(1):79–93. https://doi.org/10.1175/BAMS-D-15-0004.1

Keuler K, Radtke R, Kotlarski S, Lüthi D (2016) Regional climate change over Europe in COSMO-CLM: influence of emission scenario and driving global model. Meteorol Z 25(2):121–136. https://doi.org/10.1127/metz/2016/0662

Kovats RS, Valentini R, Bouwer LM, Georgopoulou E, Jacob D, Martin E, Rounsevell M, Soussana JF (2014) Europe. In: Barros VR, Field CB, Dokken DJ, Mastrandrea MD, Mach KJ, Bilir TE, Chatterjee M, Ebi KL, Estrada YO, Genova RC, Girma B, Kissel ES, Levy AN, MacCracken S, Mastrandrea PR, White LL (eds) Climate change 2014: impacts, adaptation, and vulnerability. Part B: regional aspects. Contribution of working group II to the fifth assessment report of the intergovernmental panel on climate change. Cambridge University Press, Cambridge, United Kingdom and New York, NY, USA, pp 1267–1326

Kröner N, Kotlarski S, Fischer E et al (2017) Separating climate change signals into thermodynamic, lapse-rate and circulation effects: theory and application to the European summer climate. Clim Dyn 48:3425–3440. https://doi.org/10.1007/s00382-016-3276-3

La Barbera P, Lanza LG, Stagi L (2002) Tipping bucket mechanical errors and their influence on rainfall statistics and extremes. Water Sci Technol 45:1–10

Lin X, Randall DA, Fowler LD (2000) Diurnal variability of the hydrologic cycle and radiative fluxes: comparisons between observations and a GCM. J Clim 13:4159–4179

Liu C, Ikeda K, Rasmussen R, Barlage M, Newman AJ, Prein AF et al (2017) Continental-scale convection-permitting modeling of the current and future climate of North America. Clim Dyn 49(1–2):71–95. https://doi.org/10.1007/s00382-016-3327-9

Moss RH, Edmonds JA, Hibbard KA, Manning MR, Rose SK et al (2010) The next generation of scenarios for climate change research and assessment. Nature 463:747–756

Nabat P, Somot S, Cassou C, Mallet M, Michou M, Bouniol D, Decharme B, Drugé T, Roehrig R, Saint-Martin D (2020) Modulation of radiative aerosols effects by atmospheric circulation over the Euro-Mediterranean region. Atmos Chem Phys 20(14):8315–8349. https://doi.org/10.5194/acp-20-8315-2020

Nesbitt S, Zipser EJ (2003) The diurnal cycle of rainfall and convective intensity according to three years of TRMM measurements. J Clim 16:1456–1475

Petch JC (2006) Sensitivity studies of developing convection in a cloud-resolving model. Q J R Meteor Soc 132:345–358

Pontoppidan BM, Reuder J, Mayer S, Kolstad EW (2017) Downscaling an intense precipitation event in complex terrain: the importance of high grid resolution. Tellus A Dyn Meteorol Oceanogr 69(1):1271561. https://doi.org/10.1080/16000870.2016.1271561

Poujol B, Sobolowski SP, Mooney PA, Berthou S (2019) A physically based precipitation separation algorithm for convection-permitting models over complex topography. Q J R Meteorol Soc. https://doi.org/10.1002/qj.3706

Powers JG, Klemp JB, Skamarock WC, Davis CA, Dudhia J, Gill DO, Coen JL, Gochis DJ, Ahmadov R, Peckham SE, Grell GA, Michalakes J, Trahan S, Benjamin SG, Alexander CR, Dimego GJ, Wang W, Schwartz CS, Romine GS, Liu Z, Snyder C, Chen F, Barlage MJ, Yu W, Duda MG (2017) The weather research and forecasting model: overview, system efforts, and future directions. Bull Am Meteorol Soc 98:1717–1737. https://doi.org/10.1175/BAMS-D-15-00308.1

Prein AF, Gobiet A (2017) Impacts of uncertainties in European gridded precipitation observations on regional climate analysis. Int J Climatol 37:305–327. https://doi.org/10.1002/joc.4706

Prein AF, Gobiet A, Suklitsch M, Truhetz H, Awan NK, Keuler K, Georgievski G (2013) Added value of convection permitting seasonal simulations. Clim Dyn 41(9–10):2655–2677. https://doi.org/10.1007/s00382-013-1744-6

Prein AF et al (2015) A review on regional convection-permitting climate modeling: demonstrations, prospects, and challenges. Rev Geophys 53:323–361

Prein AF, Liu C, Ikeda K, Trier SB, Rasmussen RM, Holland GJ, Clark MP (2017a) Increased rainfall volume from future convective storms in the US. Nat Clim Change 7(12):880–884. https://doi.org/10.1038/s41558-017-0007-7

Prein A, Rasmussen R, Ikeda K, Liu C, Clark MP, Holland GJ (2017b) The future intensification of hourly precipitation extremes. Nat Clim Change 7:48–52. https://doi.org/10.1038/nclimate3168

Rasmussen R, Liu C, Ikeda K, Gochis D, Yates D, Chen F et al (2011) High-resolution coupled climate runoff simulations of seasonal snowfall over Colorado: a process study of current and warmer climate. J Clim 24(12):3015–3048. https://doi.org/10.1175/2010JCLI3985.1

Rasmussen R, Ikeda K, Liu C, Gochis D, Clark M, Dai A et al (2014) Climate change impacts on the water balance of the colorado headwaters: high-resolution regional climate model simulations. J Hydrometeorol 15(3):1091–1116. https://doi.org/10.1175/JHM-D-13-0118.1

Rauthe M, Steiner H, Riediger U, Mazurkiewicz A, Gratzki A (2013) A Central European precipitation climatology—part I: Generation and validation of a high-resolution gridded daily data set (HYRAS). Meterol Z 22(3):235–256. https://doi.org/10.1127/09412948/2013/0436

Rio C, Hourdin F, Grandpeix J-Y, Lafore J-P (2009) Shifting the diurnal cycle of parameterized deep convection over land. Geophys Res Lett 36:L07809. https://doi.org/10.1029/2008GL036779

Roberts NM (2003) Stage 2 report form the storm-scale numerical modelling project. Technical Report 407, MetOffice R&D

Rockel B, Will A, Hense A (2008) The regional climate model COSMO-CLM (CCLM). Meteorologische Zeitschrift Meteor Z 17:347–348. https://doi.org/10.1127/0941-2948/2008/0309

Schär C, Frei C, Lüthi D, Davies HC (1996) Surrogate climate-change scenarios for regional climate models. Geophys Res Lett 23(6):669–672. https://doi.org/10.1029/96GL00265

Tabary P, Dupuy P, L'Henaff G et al (2012) A 10-year (1997–2006) reanalysis of quantitative precipitation estimation over France: methodology and first results. IAHS Publ. 351:255–260

Taylor KE, Stouffer RJ, Meehl GA (2012) An overview of CMIP5 and the experiment design. Bull Am Meteorol Soc 93:485–498. https://doi.org/10.1175/BAMS-D-11-00094.1

Torma C, Giorgi F, Coppola E (2015) Added value of regional climate modeling over areas characterized by complex terrain precipitation over the Alps. J Geophys Res Atmos 120:3957–3972. https://doi.org/10.1002/2014JD022781

Wallace JM (1975) Diurnal variations in precipitation and thunderstorm frequency over the conterminous United States. Mon Weather Rev 103:406–419

Wuest M, Frei C, Altenho A, Hagen M, Litschi M, Schär C (2010) A gridded hourly precipitation dataset for Switzerland using rain-gauge analysis and radar-based disaggregation. Int J Climatol 30:1764–1775

Authors and Affiliations

Emanuela Pichelli[1] · **Erika Coppola[1]** · **Stefan Sobolowski[2]** · **Nikolina Ban[3]** · **Filippo Giorgi[1]** · **Paolo Stocchi[4]** · **Antoinette Alias[5]** · **Danijel Belušić[6]** · **Segolene Berthou[7]** · **Cecile Caillaud[5]** · **Rita M. Cardoso[8]** · **Steven Chan[7,9]** · **Ole Bøssing Christensen[10]** · **Andreas Dobler[11]** · **Hylke de Vries[12]** · **Klaus Goergen[13]** · **Elizabeth J. Kendon[7]** · **Klaus Keuler[14]** · **Geert Lenderink[12]** · **Torge Lorenz[2]** · **Aditya N. Mishra[15]** · **Hans-Juergen Panitz[16]** · **Christoph Schär[17]** · **Pedro M. M. Soares[8]** · **Heimo Truhetz[15]** · **Jesus Vergara-Temprado[17]**

[1]   The Abdus Salam International Centre for Theoretical Physics (ICTP), Trieste, Italy

[2]   NORCE Norwegian Research Centre, Bjerknes Centre for Climate Research, Bergen, Norway

[3]   University of Innsbruck (UIBK), Innsbruck, Austria

[4]   Institute of Atmospheric Sciences and Climate, National Research Council of Italy, CNR-ISAC, Bologna, Italy

[5]   CNRM, Université de Toulouse, Météo-France, CNRS, Toulouse, France

[6]   Swedish Meteorological and Hydrological Institute (SMHI), Norrköping, Sweden

[7]   Met Office Hadley Centre, Exeter, UK

[8]   Instituto Dom Luiz, Faculdade de Ciências, Universidade de Lisboa, Lisbon, Portugal

[9]   Newcastle University, Newcastle, UK

[10]   Danish Meteorological Institute (DMI), Copenhagen, Denmark

[11]   The Norwegian Meteorological Institute, Oslo, Norway

[12]   Royal Netherlands Meteorological Institute (KNMI), De Bilt, The Netherlands

[13]   Institute of Bio- and Geosciences (IBG-3, Agrosphere), Research Centre Jülich, Jülich, Germany

[14]   Brandenburg University of Technology Cottbus-Senftenberg, Cottbus, Germany

[15]   Wegener Center for Climate and Global Change (WEGC), University of Graz, Graz, Austria

[16]   Karlsruhe Institute of Technology (KIT), Institute of Meteorology and Climate Research (IMK-TRO), Karlsruhe, Germany

[17]   Institute for Atmospheric and Climate Science, ETH-Zurich, Zurich, Switzerland